Pan-genome analysis identifies intersecting roles for *Pseudomonas* specialized metabolites in potato pathogen inhibition

Alba Pacheco-Moreno[1†], Francesca L. Stefanato[1†], Jonathan J. Ford[1], Christine Trippel[1], Simon Uszkoreit[1], Laura Ferrafiat[1], Lucia Grenga[1], Ruth Dickens[1], Nathan Kelly[1], Alexander D. H. Kingdon[1], Liana Ambrosetti[1], Sergey A. Nepogodiev[2], Kim C. Findlay[3], Jitender Cheema[4], Martin Trick[4], Govind Chandra[1], Graham Tomalin[5], Jacob G. Malone[1,6]* and Andrew W. Truman[1]*

1. Department of Molecular Microbiology, John Innes Centre, Norwich, NR4 7UH, United Kingdom
2. Department of Biochemistry and Metabolism, John Innes Centre, Norwich, NR4 7UH, United Kingdom
3. Department of Cell and Developmental Biology, John Innes Centre, Norwich, NR4 7UH, United Kingdom
4. Department of Computational and Systems Biology, John Innes Centre, Norwich, NR4 7UH, United Kingdom
5. VCS Potatoes, 2 Burnt Cottages, Badingham Road, Framlingham, Suffolk, IP13 9HX, United Kingdom
6. School of Biological Sciences, University of East Anglia, Norwich, NR4 7TU, United Kingdom

[†]These authors contributed equally to this work.

***Corresponding authors**

andrew.truman@jic.ac.uk; jacob.malone@jic.ac.uk

Abstract

Agricultural soil harbors a diverse microbiome that can form beneficial relationships with plants, including the inhibition of plant pathogens. *Pseudomonas* spp. are one of the most abundant bacterial genera in the soil and rhizosphere and play important roles in promoting plant health. However, the genetic determinants of this beneficial activity are only partially understood. Here, we genetically and phenotypically characterize the *Pseudomonas fluorescens* population in a commercial potato field, where we identify strong correlations between specialized metabolite biosynthesis and antagonism of the potato pathogens *Streptomyces scabies* and *Phytophthora infestans*. Genetic and chemical analyses identified hydrogen cyanide and cyclic lipopeptides as key specialized metabolites associated with *S. scabies* inhibition, which was supported by *in planta* biocontrol experiments. We show that a single potato field contains a hugely diverse and dynamic population of *Pseudomonas* bacteria, whose capacity to produce specialized metabolites is shaped both by plant colonization and defined environmental inputs.

Introduction

Plant pathogenic microorganisms are responsible for major crop losses worldwide and represent a substantial threat to food security. Potato scab is one of the main diseases affecting potato quality (1), and presents a significant economic burden to farmers around the world. The Gram-positive bacterium *Streptomyces scabies*, which is the causal organism of potato scab, is ubiquitous and presents a threat in almost all soils (2, 3). Properly managed irrigation is a reasonably effective control measure for potato scab. However, scab outbreaks still regularly occur in irrigated soil, and with increasing pressures on water use it is clear that alternative approaches to the control of scab are needed. An attractive potential alternative involves the exploitation of soil microorganisms that suppress or kill plant pathogens, known as biocontrol agents (4, 5).

Many soil-dwelling *Pseudomonas* species form beneficial relationships with plants, positively affecting nutrition and health (6-8) and exhibiting potent antagonistic behavior towards

54 pathogenic microorganisms (4, 9, 10). *Pseudomonas* influence the plant environment using a
55 diverse range of secondary metabolites (11-14) and secreted proteins (15, 16). As such,
56 *Pseudomonas* sp. have been identified as key biocontrol organisms in numerous plant-microbe
57 systems (17, 18), and these bacteria have potential applications as agricultural biocontrol
58 agents and biofertilizers (4, 19). Many soil pseudomonads belong to the *P. fluorescens* group,
59 which consists of over 50 sub-species and exhibits huge phenotypic and genetic diversity (6,
60 10, 20-22), with a core genome of about 1,300 genes and a pan-genome of over 30,000 genes
61 (23). These bacteria use a variety of mechanisms to colonize the plant rhizosphere (24),
62 communicate with plants (7), and suppress a range of plant pathogens (9), including bacteria
63 (25), fungi (26) and insects (27), although a single strain is unlikely to have all of these attributes.
64 Specialized metabolites are critical to many of these ecological functions, and the
65 *Pseudomonas* specialized metabolome is one of the richest and best characterized of any
66 bacterial genus (11-13).
67
68 Various studies have associated pseudomonads with potato scab suppression. A significant
69 increase in the abundance of *Pseudomonas* taxa has been observed for irrigated fields,
70 correlating with reduced levels of potato scab (28). Naturally scab-suppressive soils have also
71 been shown to contain a greater proportion of *Pseudomonas* when compared to scab-
72 conducive soils (29, 30), and phenazine production by *P. fluorescens* can contribute to scab
73 control (14, 25, 31). Differences between soil microbial populations that enable effective
74 pathogen suppression are routinely assessed using amplicon sequencing (29, 32). However,
75 the heterogeneity of the *P. fluorescens* group limits the usefulness of these methods for
76 observing changes at the species or even the genus level. To effectively determine the
77 relationship between the soil *Pseudomonas* population and disease suppression, it is important
78 to accurately survey genotypic and phenotypic variability at the level of individual isolates, and
79 to determine how this variation is linked to agriculturally relevant environmental changes (33).
80

81 To investigate the genetic bases for *S. scabies* inhibition by *P. fluorescens* and to assess
82 whether the scab-suppressive effects of irrigation derive from increased populations of
83 biocontrol genotypes in the soil or on the plant, we focused on the *Pseudomonas* population
84 from a potato field susceptible to potato scab. We first employed a phenotype-genotype
85 correlation analysis across *P. fluorescens* strains isolated from a single potato field. We
86 hypothesized that an unbiased correlation analysis would identify genetic loci and biosynthetic
87 gene clusters that may be overlooked by screening for bioactive small molecules or by focusing
88 on the biosynthetic repertoire of a limited number of strains. Here, we correlated phylogeny,
89 phenotypes, specialized metabolism and accessory genome loci, then investigated the
90 importance of strong correlations by genetic manipulation of selected wild isolates. In total, 432
91 *Pseudomonas* strains were phenotyped (with 69 whole genomes sequenced). This approach
92 also enabled us to answer a number of ancillary questions: how diverse is the *P. fluorescens*
93 population from a single field location? Do the phenotypes associated with a *P. fluorescens*
94 strain correlate with its biosynthetic capacity? What does irrigation do to both the population
95 structure of the *P. fluorescens* group and to the wider bacterial community? Using this approach,
96 we identify the *P. fluorescens* genes, gene clusters and natural products that are required for
97 potato pathogen suppression *in vitro*. We use this data to inform the discovery that the cyclic
98 lipopeptide tensin is a key determinant of *in planta* pathogen suppression by a *Pseudomonas*
99 species. We show that irrigation induces profound and repeatable changes in the microbiome,
100 both on a global level and within the *P. fluorescens* species group. Finally, we propose a model
101 for the relationship between irrigation, pathogen suppression, and population-level shifts within
102 the plant-associated *P. fluorescens* population.
103

104 ## Results

105 **Irrigation induces a significant change in the soil microbiome**

106 The ability of irrigation to protect root vegetables against *S. scabies* infection is agriculturally
107 important and widespread, but poorly understood. It is likely that the irrigated soil microbiota
108 plays a role in mediating scab suppression, but how this occurs is unclear. We therefore

assessed the impact of irrigation on the total bacterial population of a commercial potato field in the United Kingdom. Multiple soil samples were taken from two sites (A1 and B1) within this field, immediately prior to potato planting in January. Following potato planting, one site was irrigated as normal (site A), while the second was protected from irrigation (site B). Tuber-associated soil was sampled from both sites in May (A2 and B2) when tubers were just forming, and the plants were most susceptible to *S. scabies* infection. Total genomic DNA was then extracted from replicate samples of each site after each sampling event, and 16S rRNA amplicon sequencing was used to examine the bacterial population in each of these sites (Figure 1, Figure S1).

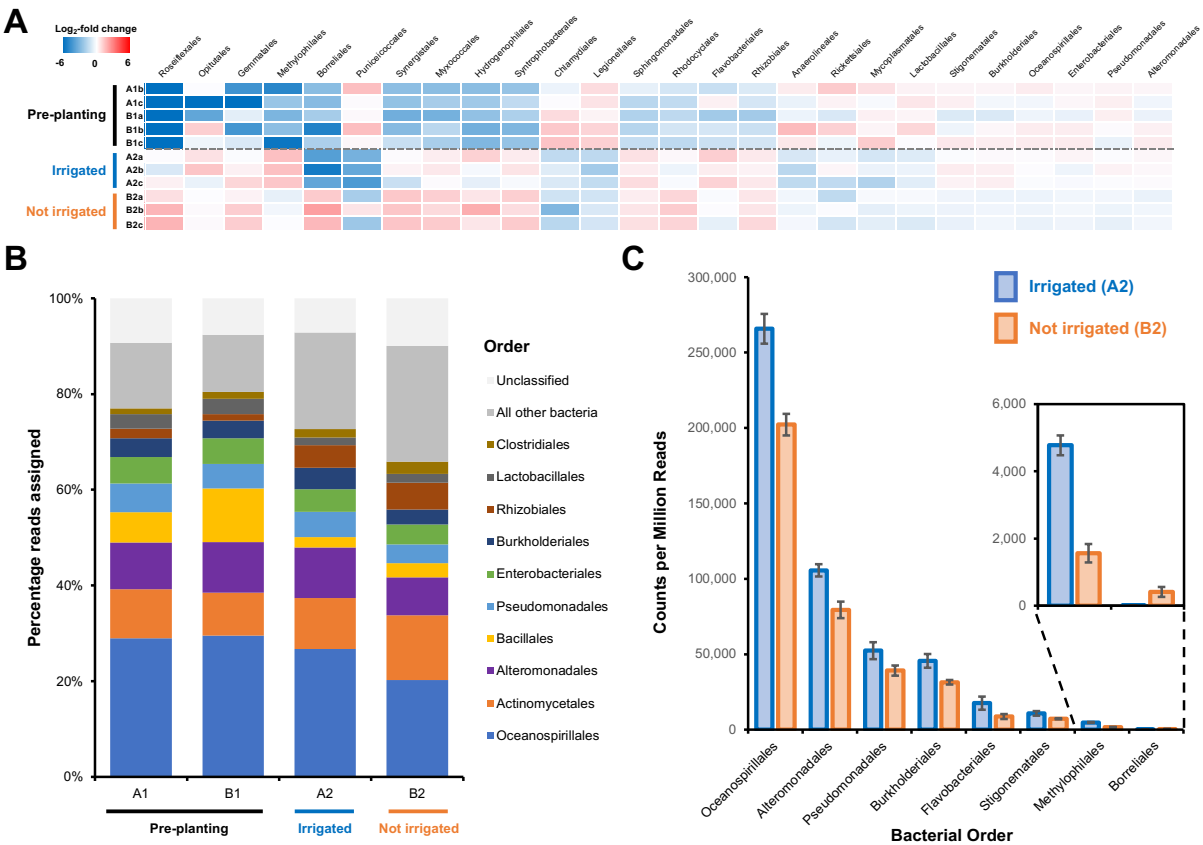

Figure 1 Effect of irrigation on the microbial population of a potato field. (A) The 26 bacterial orders whose populations were determined to significantly differ across one or more sampling sites using voom with a false discovery rate of 0.05. Data is shown as a heatmap of the $\log_2$-fold change with respect to the overall average counts per million for a given order. Sample A1a was omitted from the analysis due to possible contamination leading to an atypical bacterial population (Figure S1). (B) Overall average

125 population of each sample site showing the 10 most abundant bacterial orders across all sites. (C) The
126 eight bacterial orders whose populations were determined to significantly differ between irrigated and
127 non-irrigated sites, represented as counts per million reads. Error bars represent the standard deviation
128 of triplicate data.
129
130 We used voom (34) with a false discovery rate (FDR) of 0.05 to assess population changes
131 across the four sampling sites. In total, changes were observed for 26 bacterial orders (Figure
132 1A), with the most significant changes observed between January and May regardless of
133 irrigation. This partially reflects an increase in bacterial orders that have previously been
134 associated with the potato root microbiome (35, 36), including *Rhizobiales*, *Sphingomonadales*
135 and *Flavobacteriales*. Significant population changes (FDR<0.05) were also observed for 8
136 bacterial orders between the irrigated (A2) and non-irrigated (B2) sites (Figure 1B and 1C),
137 including a larger proportion of *Pseudomonadales* bacteria in the irrigated site. In contrast,
138 despite the potential for microbial heterogeneity across the fertilized field prior to planting, no
139 significant changes were observed between pre-planting sites A1 and B1.
140
141 **Phenotypic, phylogenetic and genomic analysis of the *P. fluorescens* field population**
142 Taxonomic identifications using 16S rRNA amplicon analysis showed order-level changes to
143 the field microbiome between sites (Figure S1) but were unable to accurately capture diversity
144 within genera or species groups. Therefore, biologically relevant variation within the populations
145 of genetically diverse species groups such as *P. fluorescens* is potentially overlooked. To
146 investigate the diversity of the fluorescent pseudomonad population, we isolated 240 individual
147 *Pseudomonas* strains from our pre- and post-irrigation field sites (Supporting Dataset 1). These
148 strains were screened for multiple phenotypes including motility, protease production,
149 fluorescence (siderophore production) and on-plate suppression of *S. scabies* using a cross-
150 streak assay (Figures S2 and S3). Each phenotype was scored on an ordinal scale between 0
151 (no phenotype observed) and 3 (strong phenotype). The cross-streak assay provided a rapid
152 read-out of bacterial antagonism for both contact-dependent and diffusible mechanisms of

153 growth inhibition. On-plate suppression of *S. scabies* was a surprisingly rare trait, with 79% of
154 *Pseudomonas* isolates out-competed by *S. scabies* in this assay. To determine whether this
155 suppressive activity correlated with specific genetic loci, 69 isolates were selected for whole
156 genome sequencing, where almost half (32 strains) exhibited on-plate suppression of *S. scabies*
157 and the remaining strains represented a diverse selection (based on phenotypic variation and
158 16S rRNA sequencing) of non-suppressive strains. We hypothesized that a comparative
159 analysis of a similar number of genomes from suppressive and non-suppressive strains would
160 identify those biosynthetic gene clusters (BGCs) that play important roles in suppressive activity.
161
162 The phylogeny of the 69 sequenced strains was analyzed alongside various model
163 pseudomonads, including representatives of the eight phylogenomic *P. fluorescens* groups
164 defined by Garrido-Sanz *et al.* (23). Our sequenced strain collection spans much of this
165 characterized global phylogenetic diversity and contains representatives of at least five of the
166 eight *P. fluorescens* phylogenomic groups (23), as well as strains belonging to the *P. putida* and
167 *P. syringae* groups (Figure S4). This genetic heterogeneity was also reflected in the diverse
168 specialized metabolome of these strains, as predicted by a detailed analysis of the BGCs
169 encoded in their genomes. Each genome was subjected to antiSMASH 5.0 analysis (37), which
170 was further refined by extensive manual annotation to improve the accuracy of predicted
171 pathway products. This second annotation step was particularly important for BGCs that are
172 atypically distributed across two distinct genomic loci (e.g. viscosin and pyoverdine). Our
173 analysis was further expanded to include BGCs not identified by antiSMASH 5.0, including
174 BGCs for hydrogen cyanide (HCN) (38), microcin B17-like pathways (39) and the auxin indole-
175 3-acetic acid (IAA) (40, 41). This was achieved by searching the genomes with a curated set of
176 known *Pseudomonas* BGCs using MultiGeneBlast (42) (see Supplementary Information for
177 further details). This manual annotation provided a level of resolution superior to that provided
178 by automated cluster-searching algorithms alone and provided confidence that the majority of
179 natural product biosynthetic potential had been identified. Within a given pathway type (e.g.
180 non-ribosomal peptide synthetases, NRPSs), likely pathway products were assigned where

181 possible (e.g. cyclic lipopeptides, CLPs) or assigned a code when a conserved uncharacterized

182 BGC was identified (e.g. NRPS 1). All BGCs were mapped to strain phylogeny (Figure 2).

183

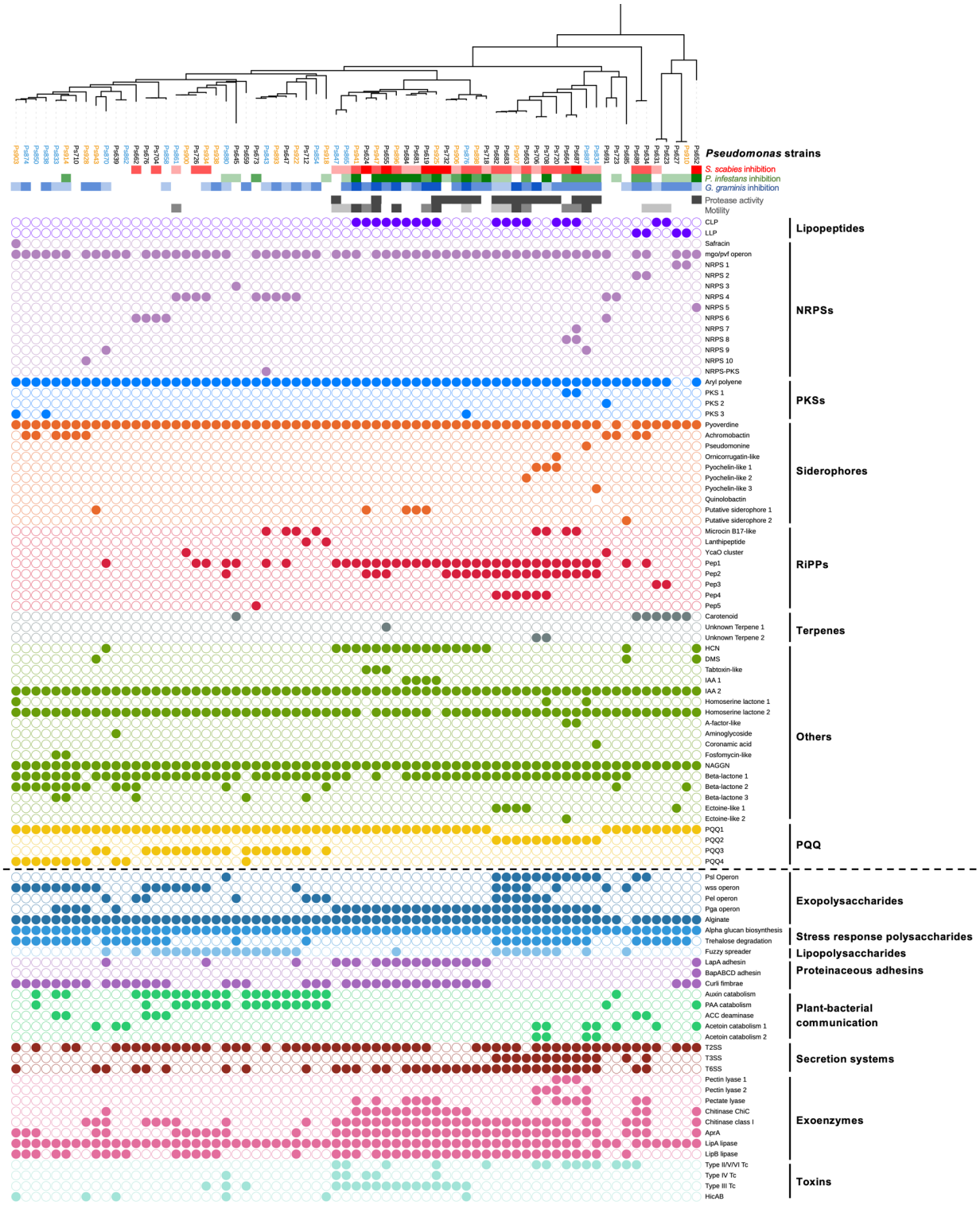

184

185 **Figure 2** Comparison of phylogeny, *S. scabies* suppression (red colour scales), *P. infestans*

186 suppression (green colour scale), *G. graminis* pv. *tritici* (take-all) suppression (blue colour scale),

187 phenotypes (grey colour scales), natural product biosynthetic gene clusters (filled circles = presence of a
188 gene or gene cluster) and the accessory genome (separated from BGCs by a dotted line). In the
189 phylogenetic tree of *Pseudomonas* strains, blue strains were collected from irrigated plots while orange
190 strains were collected from unirrigated plots. All other strains were collected from the pre-irrigation plots.
191 Figure S4 shows the relationship between these strains and the *Pseudomonas* phylogenomic groups
192 defined by Garrido-Sanz *et al.* (23).
193
194 Multiple BGCs were commonly found across the sequenced strains (Figure 2, Supporting
195 Dataset 1), including BGCs predicted to make CLPs (43), arylpolyenes (44) and HCN (38). In
196 addition to pyoverdine BGCs (45) in almost all strains, numerous other siderophore BGCs were
197 identified, including pathways predicted to make achromobactin (46), ornicorrugatin (47),
198 pyochelin-like molecules (48) (Figure S5) and a pseudomonine-like molecule (49). A variety of
199 polyketide synthase (PKS), terpene and NRPS BGCs with no characterised homologues were
200 also identified (Figure 2). Furthermore, BGCs were identified that were predicted to make
201 compounds related to microcin B17 (39), fosfomycin-like antibiotics (50), lanthipeptides (51),
202 safracin (52), a carbapenem (53) and an aminoglycoside (54) (Figure S6). Each of these natural
203 product classes is predicted to have potent biological activity and some are rarely found in
204 pseudomonads.
205
206 In addition to these potentially antibacterial and cytotoxic compounds, all genomes contain
207 BGCs predicted to produce the plant auxin IAA, while 23 genomes contained genes for IAA
208 catabolism (55). All 69 strains had at least one BGC for the production of the electron-transport
209 cofactor pyrroloquinoline quinone (56) (PQQ, Figure S7), reported to function as a plant growth
210 promoter (57). Surprisingly, BGCs for numerous well characterized *Pseudomonas* specialized
211 metabolites were not found, including phenazine, pyrrolnitrin or 2,4-diacylphloroglucinol BGCs
212 (11). In total, 787 gene clusters were identified that could be sub-divided into 61 gene cluster
213 families (Figure 2).
214

215 The *P. fluorescens* species group possesses a highly diverse array of non-essential accessory
216 genes and gene clusters. These are often critical to the lifestyle of a given strain, and can include
217 motility determinants, proteases, secretion systems, polysaccharides, toxins and metabolite
218 catabolism pathways (17). These accessory genome loci were identified using MultiGeneBlast
219 (details in Supplementary Information), which revealed a high degree of genomic diversity
220 across strains. Specialized metabolism BGCs and accessory genome loci were mapped to
221 strain phylogeny (Figure 2), which indicated that for some loci (e.g. the *psl* operon, auxin
222 catabolism, HCN biosynthesis) there is a close, but not absolute, relationship between
223 phylogeny and the presence of a gene cluster.
224

225 **Correlation analysis identifies potential genetic determinants of *S. scabies* inhibition**

226 We hypothesised that genes associated with suppression of *S. scabies* could be identified by a
227 correlation analysis between *S. scabies* cross-streak inhibition and the presence of BGC
228 families or accessory genes. We therefore calculated Pearson correlation coefficients for each
229 BGC with *S. scabies* inhibition (Figure S8). The top 10 positively correlating genotypes and
230 phenotypes (Figure 3) comprised four BGC families (Pep1, CLP, Pep2 and HCN) (Figure S9),
231 four accessory genome loci (chitinase ChiC, protease AprA, chitinase class 1 and the Pga
232 operon) and two phenotypes (motility and secreted protease production). The production of
233 HCN and/or CLPs by *Pseudomonas* strains have been previously associated with the
234 suppression of various plant pathogens including fungi (26, 58) and oomycetes (59, 60), and
235 can also contribute to insect killing (27, 61), but have not been linked to the suppression of
236 bacteria. A variety of genotypes associated with plant-microbe interactions were moderately
237 negatively correlated with suppression ($\rho < -0.3$), including BGCs for PQQ biosynthesis and
238 catabolism of the plant auxins IAA and phenylacetic acid (PAA) (Figure 3A).

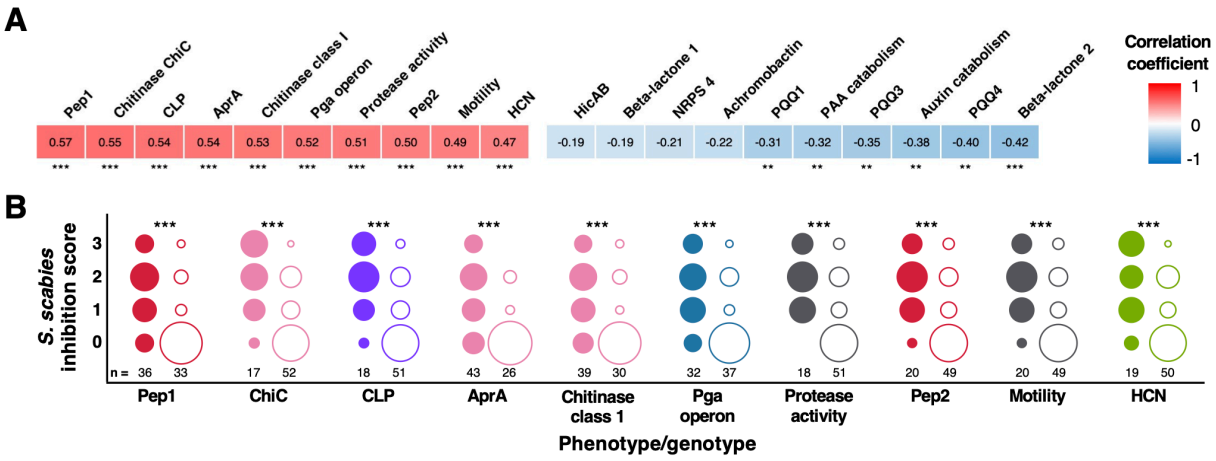

Figure 3 Correlation of BGCs and accessory genome loci with *S. scabies* inhibition. (A) Heatmap showing the 10 genotypes and phenotypes that correlated most strongly (positively and negatively) with on-plate suppression of *S. scabies*. Stars represent the statistical significance of a correlation using a two-tailed Mann-Whitney test ($p<0.05$ = *, $p<0.01$ = **, $p<0.001$ = ***). (B) Distributions of *S. scabies* suppressive activity for top 10 positive correlations. Circles are stacked from no (0) to high (3) inhibition, where filled and empty circles represent strains with and without a given genotype/phenotype, respectively. The number of strains (total = 69) in each class is listed, and the area of a circle specifies the proportion of strains with given suppressive activity.

Interestingly, while certain BGC loci (e.g. CLP) positively correlated with both suppression and motility, this relationship was not seen for every locus (e.g. HCN correlates with suppression but is less strongly correlated with motility). Correlation does not equate to causation, especially considering the significant evolutionary association seen for some BGCs (Figure 3C). The importance of correlating BGCs to *S. scabies* suppression was therefore investigated experimentally using a genetically tractable subset of suppressive isolates.

Production and role of CLPs in suppression of *S. scabies*

The strong positive correlation between putative CLP gene clusters and *S. scabies* suppression prompted us to investigate whether CLPs play a role in suppressive activity. *Pseudomonas* CLPs have previously been associated with a wide array of functions, including fungal growth inhibition, plant colonisation and promotion of swarming motility (43, 62), although there are no

261 reports of *Pseudomonas* CLPs functioning as inhibitors of streptomycete growth. However, prior
262 work has shown that surfactin, a CLP from *Bacillus subtilis,* inhibits *Streptomyces coelicolor*
263 aerial hyphae development (63), while iturin A, a CLP from *Bacillus* sp. sunhua, inhibits *S.*
264 *scabies* development (64).
265
266 To determine the identity of each CLP we combined bioinformatic predictions of the NRPS
267 products (37) with experimental identification using liquid chromatography – tandem mass
268 spectrometry (LC-MS/MS). In every strain that contained a CLP BGC, a molecule with an
269 expected mass and MS/MS fragmentation pattern was identified (Figure 4, Figures S10-S16).
270 This showed that *P. fluorescens* strains from a single field have the collective capacity to make
271 viscosin (*m/z* 1126.69, identical retention time to a viscosin standard) (65), a viscosin isomer
272 (*m/z* 1126.69, different retention time to viscosin standard) (Figures S10 and S11), as well as
273 compounds with BGCs, exact masses and MS/MS fragmentation consistent with tensin (*m/z*
274 1409.85, Figure S12) (66), anikasin (*m/z* 1354.81, Figure S13) (67), and putisolvin II (*m/z*
275 1394.85, Figure S14) (68). In addition, an array of related metabolites were observed that
276 differed by 14 or 28 Da, which is characteristic of different lipid chain lengths. This analysis also
277 proved that the linear lipopeptides syringafactin A (*m/z* 1082.74) and cichofactin (*m/z* 555.38,
278 $[M+2H]^{2+}$) were made by strains harbouring BGCs predicted to make these phytotoxins (69, 70)
279 (Figures S15 and S16). The metabolic capacity of all strains was mapped using mass spectral
280 networking (71, 72), which showed that CLPs were strongly associated with strains that inhibit
281 *S. scabies* (Figure 4).
282

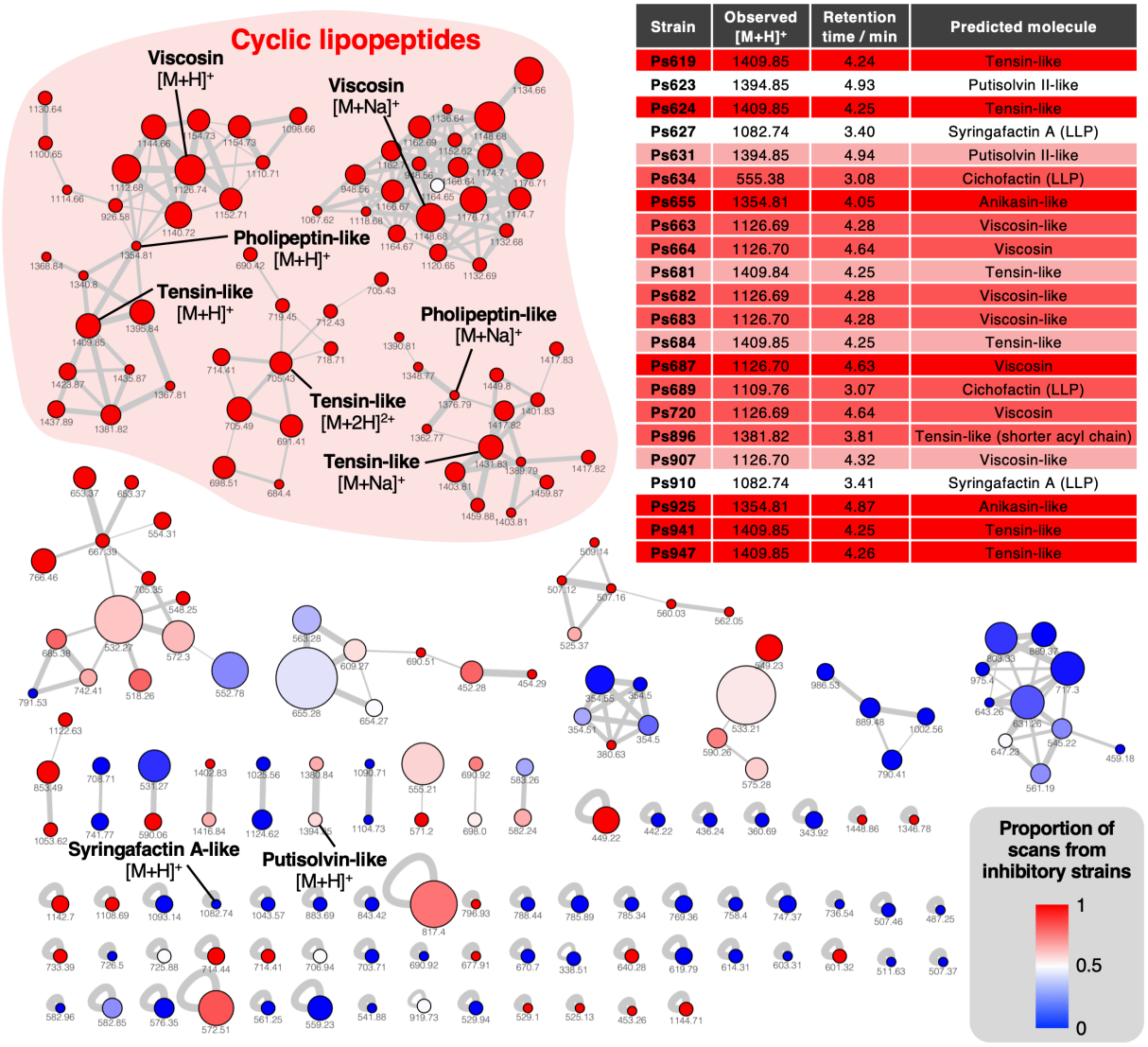

Strain	Observed [M+H]+	Retention time / min	Predicted molecule
Ps619	1409.85	4.24	Tensin-like
Ps623	1394.85	4.93	Putisolvin II-like
Ps624	1409.85	4.25	Tensin-like
Ps627	1082.74	3.40	Syringafactin A (LLP)
Ps631	1394.85	4.94	Putisolvin II-like
Ps634	555.38	3.08	Cichofactin (LLP)
Ps655	1354.81	4.05	Anikasin-like
Ps663	1126.69	4.28	Viscosin-like
Ps664	1126.70	4.64	Viscosin
Ps681	1409.84	4.25	Tensin-like
Ps682	1126.69	4.28	Viscosin-like
Ps683	1126.70	4.28	Viscosin-like
Ps684	1409.85	4.25	Tensin-like
Ps687	1126.70	4.63	Viscosin
Ps689	1109.76	3.07	Cichofactin (LLP)
Ps720	1126.69	4.64	Viscosin
Ps896	1381.82	3.81	Tensin-like (shorter acyl chain)
Ps907	1126.70	4.32	Viscosin-like
Ps910	1082.74	3.41	Syringafactin A (LLP)
Ps925	1354.81	4.87	Anikasin-like
Ps941	1409.85	4.25	Tensin-like
Ps947	1409.85	4.26	Tensin-like

Figure 4 Mass spectral networking analysis of LC-MS/MS data from the *Pseudomonas* strains used in this study. Node area is proportional to the number of distinct strains where MS/MS data was acquired for a given metabolite. Node colour reflects the proportion of MS/MS scans for a given node that come from strains with a *S. scabies* inhibition score ≥1. Nodes are labelled with the corresponding parent masses and nodes that relate to lipopeptides are labelled (multiple networks arise from differential fragmentation of $[M+H]^+$, $[M+2H]^{2+}$ and $[M+Na]^+$ ions). Line thickness is proportional to the cosine similarity score calculated by Global Natural Product Social Molecular Networking (GNPS) (72). The table shows production of lipopeptides by strains containing lipopeptide BGCs. Colour-coding reflects level of *S. scabies* inhibition by each strain with same scale as Figure 2 (LLP = linear lipopeptide; all others are CLPs).

295 To assess the potential role of CLPs in mediating the interaction between *P. fluorescens* and *S.*
296 *scabies*, an NRPS gene predicted to be involved in the biosynthesis of a viscosin-like molecule
297 in Ps682 was deleted by allelic replacement (Figure 5A). The resulting Ps682 Δ*visc* strain was
298 unable to make the viscosin-like molecule (*m/z* 1126.69, Figure 5B), or to undergo swarming
299 motility (Figure S17). This is in agreement with earlier work on the role of viscosin in the motility
300 of *P. fluorescens* SBW25 (62) and the observation that possession of a CLP BGC was the
301 genotype that most strongly correlated with motility ($\rho = 0.65$, Figure S8). A cross-streak assay
302 with *S. scabies* revealed an active role for this CLP in on-plate *S. scabies* inhibition (Figure 5D).
303 Wild type (WT) Ps682 appeared to specifically colonise the *S. scabies* streak, whereas Ps682
304 Δ*visc* was unable to restrict *S. scabies* growth. Alternatively, it was possible that this instead
305 could reflect diffusible inhibition of *Streptomyces* development by WT Ps682, leading to a "bald"
306 *S. scabies* phenotype (73). To distinguish between these possible inhibition modes, a
307 constitutively-expressed *lux* operon was integrated into the chromosomal *att::*Tn*7* site (74) of
308 Ps682 to visualise this interaction by bioluminescence. This clearly showed viscosin-dependent
309 *Pseudomonas* colonisation of the *Streptomyces* streaks (Figure 5C).
310
311 To quantitatively assess the antagonistic effect of the Ps682 CLP, it was purified and structurally
312 characterized using MS/MS (Figure S18) and nuclear magnetic resonance (NMR) spectroscopy
313 (^{1}H, ^{13}C, COSY HSQC, TOCSY, HMBC, Figures S19-S29, Table S4). NMR analysis revealed
314 that the molecule has an identical amino acid composition to viscosin (3-hydroxydecanoic acid-
315 Leu1-Glu2-Thr3-Val4-Leu5-Ser6-Leu7-Ser8-Ile9, Figure 5B), which was fully supported by
316 detailed high-resolution MS (calculated viscosin $[M+H]^+$ = 1126.6970, observed $[M+H]^+$ =
317 1126.6964) and MS/MS fragmentation data (Figure S18). The LC retention time of this CLP is
318 different to viscosin, but is almost identical to WLIP (Figure S18), which is a viscosin isomer that
319 has a D-Leu5 residue instead of L-Leu5 (75). However, comparison of NMR data in DMF-d7
320 revealed some minor shift differences between published WLIP spectra (75) and the Ps682
321 CLP, such as the γ-CH_2 group of Glu2 (WLIP = δ_H 2.54 ppm, δ_C 30.3 ppm; Ps682 CLP = δ_H
322 2.24 ppm, δ_C 34.8 ppm). Therefore, we could not conclusively confirm the absolute configuration

323 of the Ps682 CLP and thus named it viscosin I (for viscosin Isomer). A disk diffusion assay of
324 purified viscosin I with *S. scabies* (Figure 5D) demonstrated that it directly inhibited *S. scabies*
325 growth with a minimum inhibitory concentration of approximately 20 µg/mL. Long-term growth
326 of *S. scabies* in the presence of viscosin I (Figure S30) indicated that the inhibition of *S. scabies*
327 is temporary and growth partially resumes after several days. These data show that in addition
328 to its role as a surfactant, viscosin I functions by inhibiting the growth rate of *S. scabies*,
329 consistent with the on-plate data for Ps682 Δ*visc*.

330

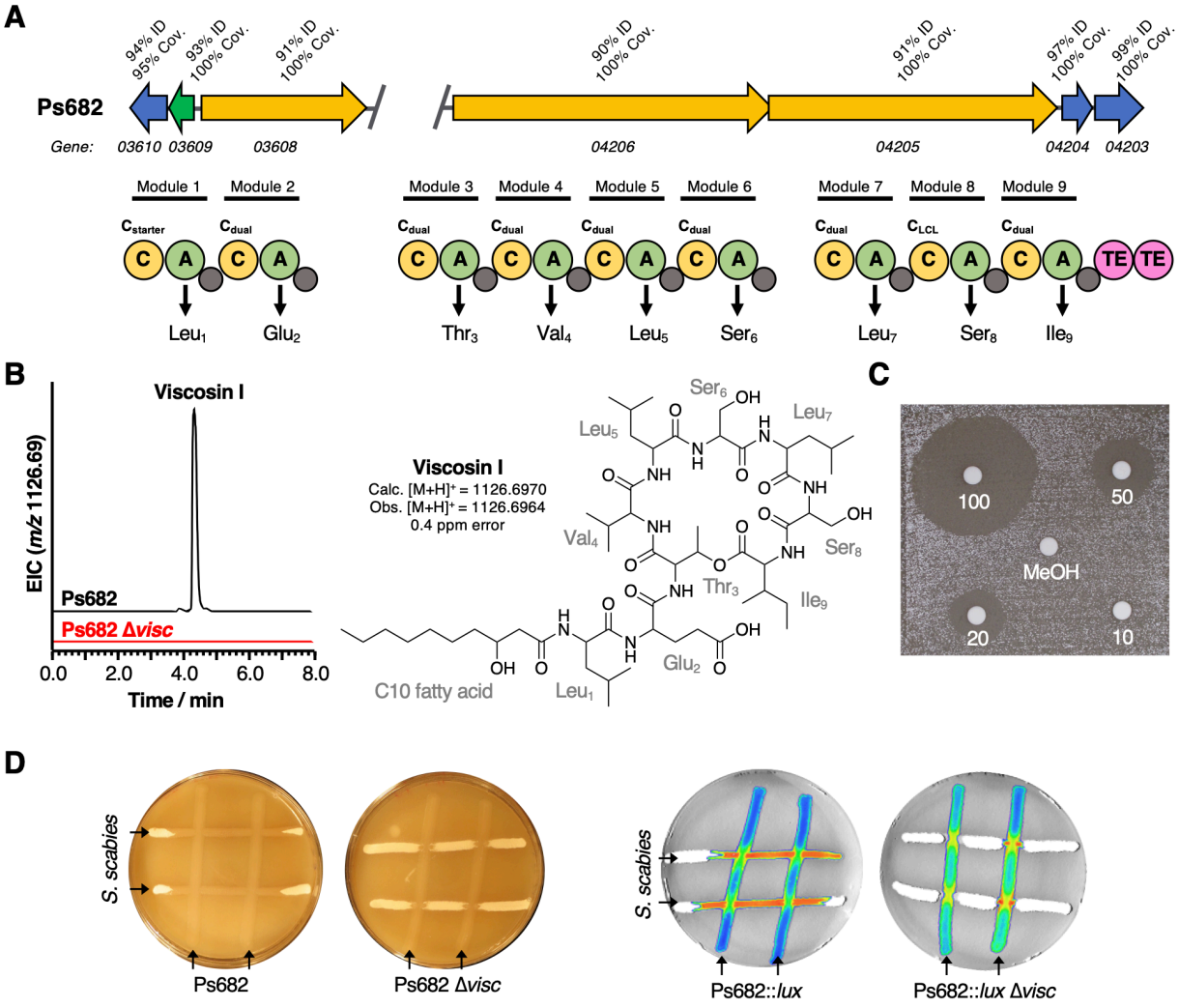

331

332 **Figure 5** The role of the Ps682 CLP BGC in *S. scabies* suppression. (A) BGC displaying
333 identity/coverage scores in comparison to the viscosin BGC in *P. fluorescens* SBW25. Genes encoding
334 regulatory proteins are green, transporter genes are blue, and NRPS genes are yellow. The NRPS
335 organization is shown, where C = condensation domain, A = adenylation domain, TE = thioesterase

336 domain, and grey circles are peptidyl carrier protein domains. Amino acids incorporated by each module
337 are displayed, along with predicted condensation domain specificity. (B) LC-MS analysis of viscosin I
338 production in the WT strain and a mutant (Ps682 Δ*visc*) with an in-frame deletion of NRPS gene 04206.
339 NMR and MS/MS data for viscosin I is shown in Figures S19-S29. (C) Disk diffusion assay of viscosin I
340 against *S. scabies*. Concentrations are indicated (µg/mL), alongside a methanol control. (D) On-plate *S.*
341 *scabies* suppression activity of Ps682 alongside Ps682 Δ*visc* shown as cross-streaks using strains with
342 and without the *lux* operon. Bioluminescence was detected using a NightOWL camera (Berthold
343 Technologies).
344

345 **HCN and CLP production both contribute to on-plate *S. scabies* inhibition**

346 Pan-genome analysis showed that HCN production was predicted for a significant number of
347 suppressive strains (ρ = 0.47, Figure S8), where 17 of the 19 strains containing HCN gene
348 clusters were inhibitory towards *S. scabies* (Figure 2). The HCN pathway is encoded by the
349 *hcnABC* gene cluster (Figure S9) and has previously been associated with insect and fungal
350 pathogen inhibition in other *Pseudomonas* strains (27) (59, 76). HCN is toxic to a wide variety
351 of organisms, but not to *Pseudomonas* owing to their branched aerobic respiratory chain that
352 has at least five terminal oxidases, including a cyanide-insensitive oxidase (77, 78). We
353 confirmed that nearly every strain with the *hcnABC* gene cluster produced HCN (18 out of 19)
354 using the Feigl-Anger colorimetric detection reagent (79) (Supporting Dataset 1) and used this
355 assay to identify HCN producers across the original collection of 240 *Pseudomonas* strains.
356 This wider analysis showed that HCN production strongly correlated with *S. scabies* inhibition
357 (ρ = 0.52, Figure S31), in accordance with our analysis of the sequenced strains.
358

359 To examine the role of HCN in *S. scabies* suppression and whether it exhibited a synergistic
360 effect with CLP production, Ps619 was investigated as this strain produces both HCN and a
361 tensin-like CLP (Figure 2 and Figure 6A). A tensin BGC has not previously been reported, but
362 the predicted amino acid specificity, mass (Figure 6A) and MS/MS fragmentation (Figure S12)
363 indicated that seven isolates produce tensin-like CLPs (Figure 4). The *hcn* and *ten* gene clusters
364 were inactivated by in-frame deletions to generate single and double mutants of Ps619, and the

365 resulting Δ*hcn*, Δ*ten* and Δ*hcn*Δ*ten* mutants were subjected to cross-streak assays (Figure 6B).
366 A comparison of wild type, single and double mutants showed that HCN inhibits *S. scabies*
367 growth and development across the entire plate, while tensin is important for *Pseudomonas*
368 motility and helps the *Pseudomonas* to grow competitively at the cross-streak interface.
369 Furthermore, this suppressive effect is additive: the Ps619 Δ*hcn* and Δ*ten* single mutants both
370 retained some inhibitory activity towards *S. scabies*, whereas the Ps619 Δ*hcn*Δ*ten* double
371 mutant could not inhibit *S. scabies*.
372

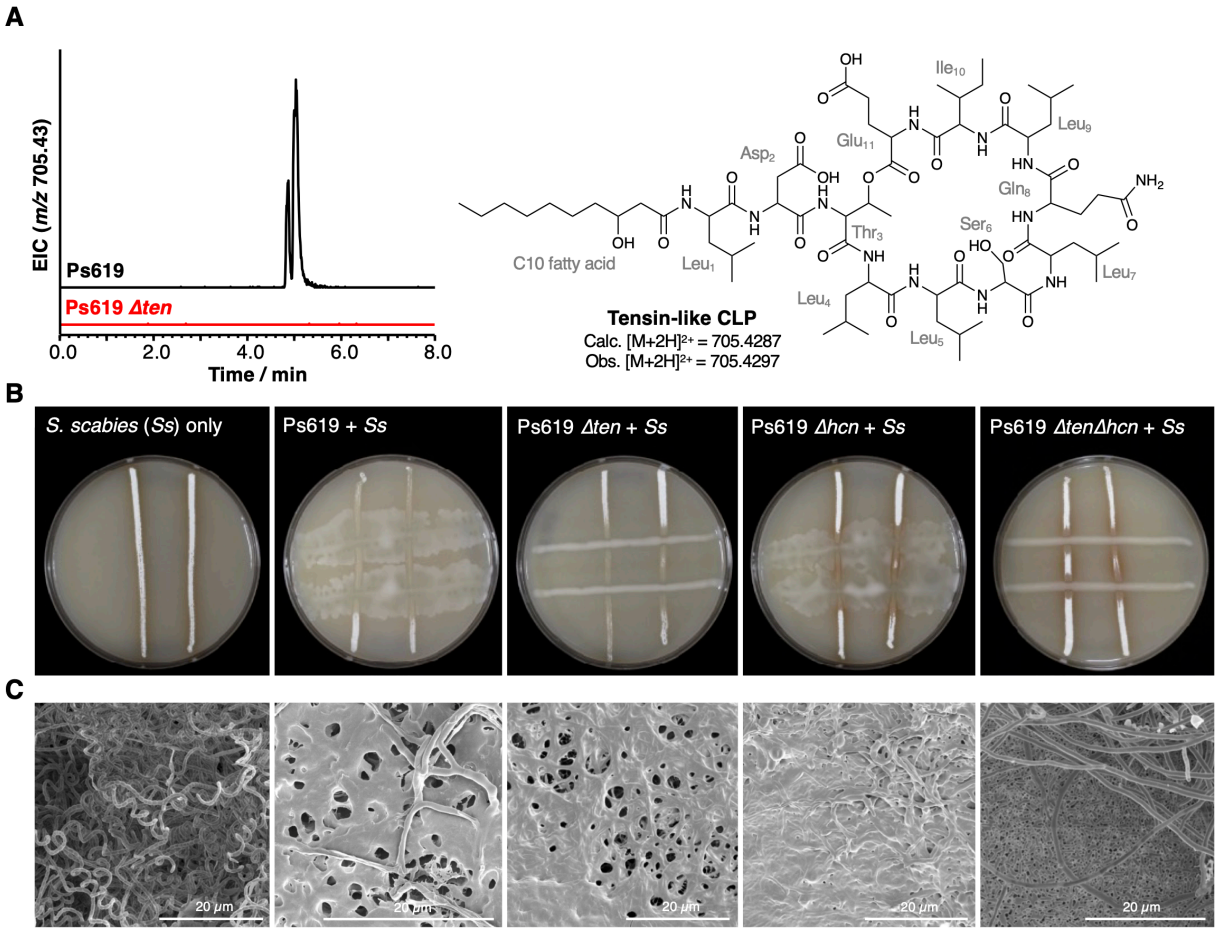

373

374 **Figure 6** The role of the Ps619 CLP and HCN gene clusters in *S. scabies* suppression. (A)
375 Predicted structure of the tensin-like molecule and LC-MS analysis of CLP production in WT Ps619 and
376 a mutant (Ps619 Δ*ten*) with an in-frame deletion of NRPS gene 02963 (see Figure S12 for BGC
377 information). (B) Cross streak assays of Ps619 and associated mutants with *S. scabies*. See Figure S32
378 for assays with drier plates. (C) Cryo-SEM images of the interfacial region between the Ps619 strains
379 and *S. scabies*. The order of images is identical to the cross-streaks in panel B.

380

381 In drier growth conditions expected to favour streptomycete growth and limit motility, the role of
382 tensin-mediated motility was abrogated, yet tensin and HCN still possessed an additive
383 inhibitory effect at the microbial interface (Figure S32). Notably, Ps619 Δ*hcn* was able to induce
384 a developmental defect in *S. scabies* at the microbial interface that was not present in Ps619
385 Δ*ten* or Ps619 Δ*hcn*Δ*ten*, showing that the tensin-like CLP induces a developmental defect in
386 *S. scabies* that is independent of *Pseudomonas* motility, comparable to the inhibitory effect of
387 isolated viscosin I. This analysis also clearly showed that at areas distant from the bacterial
388 interaction, *S. scabies* grew more vigorously when cultured with Δ*hcn* strains, consistent with
389 the volatility of HCN enabling a long-range inhibitory effect. A similar volatile effect was seen
390 when Ps619 strains were separated from *S. scabies* by a barrier, where only those strains
391 producing HCN inhibited growth and development (Figure S32).

392

393 To further probe how tensin and HCN affected the interaction between Ps619 strains and *S.*
394 *scabies*, the interfacial regions of cross-streaks were imaged using Cryo-scanning electron
395 microscopy (cryo-SEM). WT Ps619 was able to colonise the *S. scabies* streak meaning that the
396 interfacial region imaged was further from the cross-streak intersection than all other co-cultures
397 (Figure 6C). Here, Ps619 inhibited *S. scabies* development, which appears as a mixture of
398 deformed aerial hyphae and vegetative growth reminiscent of a “bald” phenotype (80). Cryo-
399 SEM indicated that both the Ps619 Δ*hcn* and Δ*ten* mutants induced a similar partially bald
400 phenotype in *S. scabies*, but the Δ*hcn*Δ*ten* double mutant was unable to trigger the same
401 developmental defect, as *S. scabies* could develop aerial mycelia close to the microbial
402 interface (Figure 6C and Figure S33). This appears as a clear boundary between Ps619
403 Δ*hcn*Δ*ten* (single cells in background, bottom right panel of Fig 6C) and *S. scabies* (hyphae in
404 the foreground). The volatile HCN can inhibit growth and development at a distance, whereas
405 CLP inhibition of development only occurs close to the microbial interface. Both inhibitory
406 mechanisms enable Ps619 to obtain a competitive advantage at the microbe-microbe interface

407 (Figure 6C and Figure S33), while the CLP also functions as a surfactant enabling Ps619
408 motility, promoting *Pseudomonas* invasion of the *Streptomyces* cross-streak.
409
410 **Tensin is a key determinant of *in planta* inhibition of potato scab**
411 To examine the *in planta* biocontrol properties of Ps619 and Ps682, and to determine the
412 contribution of HCN and CLPs to activity, potato scab suppression assays were carried out in
413 glasshouse trials. Maris Piper potatoes were infected with *S. scabies* 87-22 and scored for
414 disease severity after 16 weeks using the method of Andrade *et al*. (81). A subset of plants was
415 also treated with *Pseudomonas* spp. and associated BGC mutants. Ps619 conferred significant
416 protection against potato scab, where disease severity was reduced to levels similar to
417 uninfected control plants (Figure 7). This suppressive ability was lost for Ps619 Δ*ten* and Ps619
418 Δ*hcn*Δ*ten*, resulting in disease severity similar to scab-infected tubers. In contrast, Ps619 Δ*hcn*
419 was just as effective as WT Ps619 at suppressing potato scab, which differed from the on-plate
420 results for HCN. The significance of these results was supported by an independent *in planta*
421 biocontrol experiment, where equivalent results were obtained for each strain (Figure S34). This
422 result indicates that tensin plays an important role in the biocontrol of potato scab. In contrast
423 with its on-plate suppressive activity, potato scab assays showed no significant antagonistic
424 activity for Ps682 against *S. scabies* infection. Unfortunately, this meant that the role of viscosin
425 I could not be determined *in planta*.
426
427

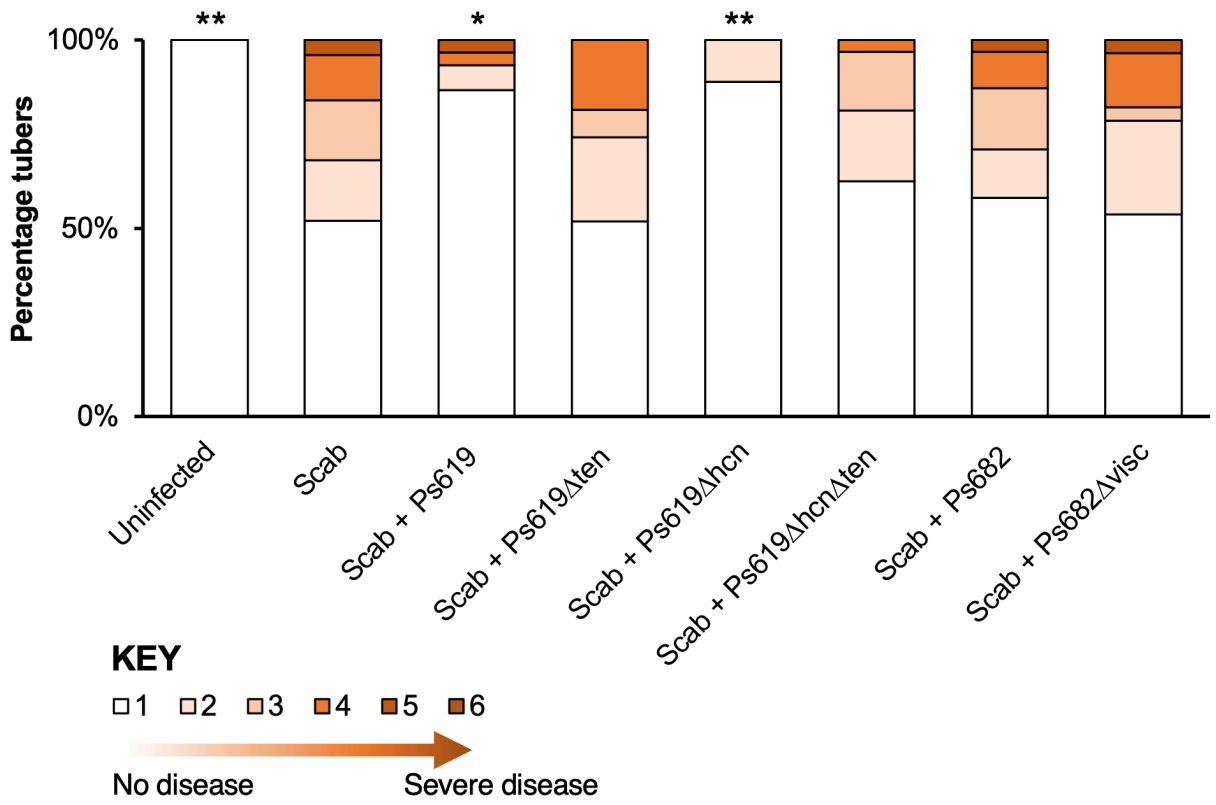

Figure 7 Potato scab biocontrol assay. The bar chart shows the percentage of diseased tubers following infection with *S. scabies* ("Scab") along with treatment by Ps619, Ps682 and associated mutants. Tubers were scored using a disease severity index from 1 to 6 according to the method of Andrade *et al*. (81). Statistical analyses were calculated by taking into account the average disease index of each plant (n=4). *p* values were calculated using Dunnett's multiple comparison test and asterisks indicate $p < 0.05$ (*), 0.01 (**) as compared to Scab treatment only. Results of a repeat biocontrol experiment and further statistical statistics are shown in Figure S34.

A subset of *P. fluorescens* strains are generalist pathogen suppressors

To determine whether the strains and metabolites we identified have suppressive activity towards a range of plant pathogens, we investigated the ability of the potato field strain collection to suppress the growth of *Phytophthora infestans*, the oomycete that causes potato blight (82), and *Gaeumannomyces graminis* var. *tritici*, the fungus that causes take-all disease of cereal crops (17). These assays revealed strong congruence between the genotypes that correlated with suppression of each pathogen (Figure S35). HCN and CLPs have both previously been identified as inhibitors of oomycete and fungal growth (26, 59). To assess whether these natural

445 products are critical for inhibition of *P. infestans* and *G. graminis* by Ps619 and Ps682, the
446 HCN/CLP mutants were tested for inhibitory activity (Figure S35). Surprisingly, neither HCN or
447 tensin were required for Ps619 inhibition of either *G. graminis* or *P. infestans* (Figure S35),
448 indicating the production of at least one other secreted inhibitory factor. In contrast, inactivation
449 of the viscosin I pathway in Ps682 abolished activity towards both pathogens (Figure 8C). These
450 data indicate that a subset of pseudomonads can function as generalist pathogen suppressors,
451 possessing multiple growth inhibition mechanisms (e.g. Ps619) and/or by producing molecules
452 with broad bioactivity (e.g. Ps682).
453
454 Multiple other genome loci are strongly correlated with pathogen suppression (Figure 3A, Figure
455 S35), including chitinases (83) and the extracellular metalloprotease AprA (84). Phenotypically,
456 extracellular protease activity also positively correlates with suppression. The BGC that
457 correlated most strongly with *S. scabies* suppression was Pep1 ("Peptide 1"), while the related
458 Pep2 also correlated strongly (Figure 3A). These were identified by antiSMASH as putative
459 "bacteriocin" BGCs, and encode short DUF2282 peptides alongside DUF692 and DUF2063
460 proteins (Figure S9). The DUF692 protein family includes dioxygenases involved in
461 methanobactin (85) and 3-thiaglutamate (86) biosynthesis. Other studies indicate that DUF692
462 and DUF2063 proteins may be involved in heavy metal and/or oxidative stress responses (87-
463 89). Further work is required to determine the significance of both the Pep BGCs and the
464 accessory genome loci for pathogen inhibition.
465
466 **The effect of irrigation on the soil *Pseudomonas* population**
467 Irrigation is currently the only effective way to control potato scab, so we hypothesised that this
468 may lead to an increase in the number of inhibitory bacteria associated with the soil and/or
469 tuber, especially as the *Pseudomonadales* population moderately increased in irrigated soil
470 (Figure 1C). However, a greater number of strongly suppressive strains (inhibition score ≥ 2)
471 were isolated from non-irrigated sites (7/60 strains) than from irrigated sites (1/60 strains). A
472 similar pattern was observed for strongly motile (score ≥ 2) strains (6 non-irrigated versus 2

473 irrigated). Analysis of the BGCs in our sequenced strains revealed a similar result, where 5/18
474 unirrigated strains contained CLP BGCs versus 0/16 irrigated strains. This counter-intuitive
475 observation led us to hypothesise that irrigation enables non-motile, non-suppressive bacteria
476 to survive and colonise plant roots, whereas highly motile bacteria that produce multiple
477 biological weapons can more effectively colonise plants in drier, more 'hostile' conditions.
478
479 To test these hypotheses, we sampled irrigated and unirrigated sites in a neighbouring field two
480 years after the first sampling event. 48 strains were isolated from bulk soil and the rhizospheres
481 of tuber-forming potato plants, with and without irrigation, providing a total of 192 *P. fluorescens*
482 strains (Supporting Dataset 1). These strains were scored for motility, HCN production and *S.*
483 *scabies* suppression (Figure 8A). Our results were in strong agreement with the first sample
484 set, including strong positive correlations between *S. scabies* inhibition, motility and HCN
485 production (Figure 8B). A negative correlation was observed between irrigation and *S. scabies*
486 suppression on the plant roots, but not in the surrounding soil. This appeared to be driven
487 primarily by differences in the unirrigated samples, where a substantially greater proportion of
488 suppressive isolates were associated with roots than with the surrounding soil. We observed a
489 strong positive correlation between motility and root association for unirrigated samples, while
490 the reverse was true for irrigated plants (Figure 8A). This effect of irrigation on the distribution
491 of motile bacteria was striking – in dry plants the motile population was almost entirely
492 associated with roots, while in irrigated plants a comparable proportion of motile bacteria were
493 found in the soil and roots (Figure 8A).

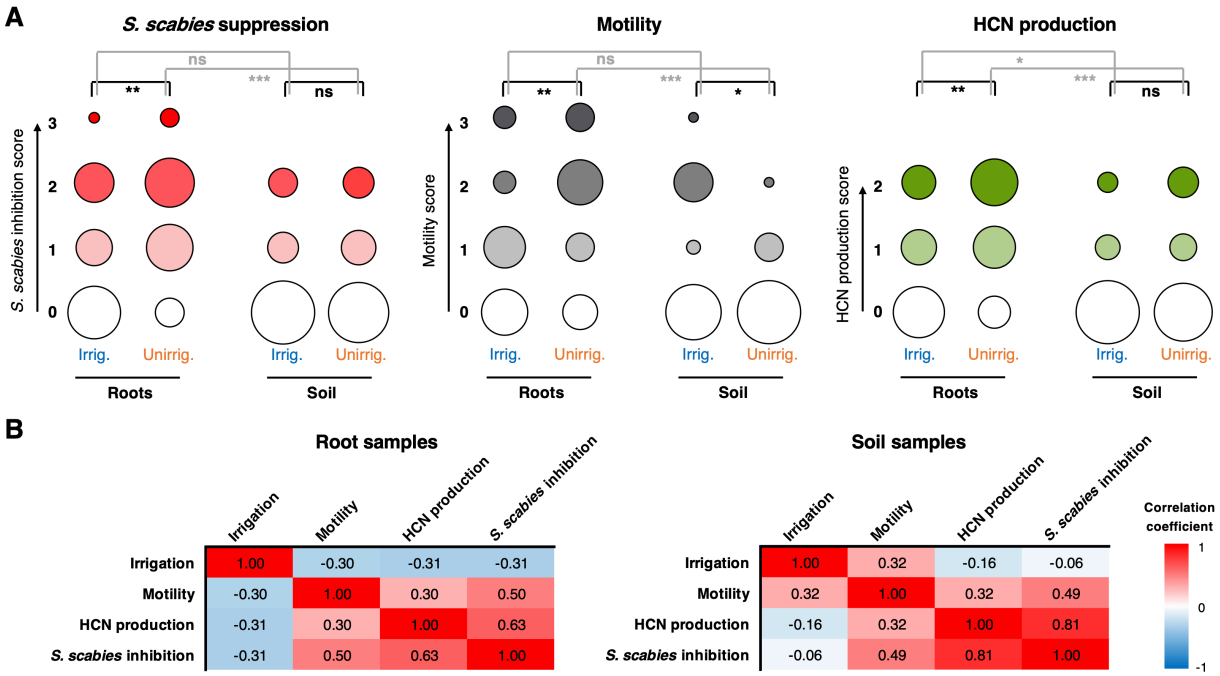

Figure 8 The effect of irrigation and environment (soil versus root) on the *P. fluorescens* population. (A) Plots showing the proportion of strains exhibiting a particular phenotype from each environment (n = 48 for each condition). HCN production was scored on a scale of 0-2 based on a qualitative assessment of the colour change in the Feigl-Anger assay. The size of each circle is proportional to the number of strains with a given phenotypic score. Statistical comparisons were carried out two-tailed Mann-Whitney tests where ns (not significant) = p≥0.05, * = p<0.05, ** = p<0.01, *** = p<0.001. (B) Pearson correlation scores for phenotypes from strains isolated from roots (n = 96) and soil (n = 96).

This analysis therefore supports the root colonisation hypothesis, where a lack of irrigation leads to a more specialized pseudomonad population colonising the root. Upon irrigation, the difference between the bulk soil and root pseudomonad populations is much less significant. The mechanism for this population change is not yet defined and these changes are counter-intuitive in relation to the suppression of potato scab upon irrigation, given there is a drop in suppressive strains colonising the potato root following irrigation. Irrigation did lead to moderately more motile pseudomonads in bulk soil versus unirrigated conditions, but this was not associated with more suppressive strains or HCN producers (Figure 8A, 8B). The

513 mechanism and significance of this irrigation effect requires further investigation. It is possible
514 that a protective microbiome in irrigated conditions actually contains a mixture of *S. scabies*-
515 suppressive "biocontrol" *Pseudomonas* strains alongside other non-motile pseudomonads that
516 interact with the plant in important ways due to traits usually absent from the "biocontrol" strains,
517 such as their ability to produce PQQ and catabolise auxins (55, 57). Profound irrigation-
518 associated changes in antibiotic-producing *Pseudomonas* populations have previously been
519 observed for the wheat rhizosphere (90, 91).
520

521 **Discussion**

522 Prior studies on the suppression of potato scab have indicated a potential biocontrol role for
523 *Pseudomonas* bacteria (14, 25, 28, 29). Fluorescent pseudomonads form multiple beneficial
524 relationships with plants, including growth promotion and biocontrol (7, 9). However, there is
525 limited understanding of the genetic factors that are critical for such activity, and little is known
526 about the diversity of the *P. fluorescens* species group within a given agricultural field or how
527 this population is shaped by environmental changes. In this study, we integrated genomics,
528 metabolomics, phenotypic analysis, molecular biology and *in planta* assays to identify the
529 genetic determinants of *Pseudomonas* antagonism towards *S. scabies*. This population level
530 approach shows that the *P. fluorescens* population in a single field is highly complex,
531 heterogeneous and dynamic (Figures 2, 3 and 8), where the overall genotypic diversity is similar
532 to the global diversity of *P. fluorescens* (23). Pan-genome analysis and metagenomics
533 represent increasingly powerful routes to understanding the genetic determinants of biological
534 activity in plant-associated microbes (10, 22, 92-95).
535

536 Multiple BGCs and accessory genome loci were identified that correlated with on-plate inhibition
537 of *S. scabies* growth and development (Figure 3), including BGCs for CLPs and HCN. These
538 loci also correlated with inhibition of *P. infestans* and *G. graminis*, and their contribution to
539 suppression was validated genetically. This confirmed a role for both molecules in *S. scabies*
540 inhibition (Figures 5 and 6), representing a new function for these *Pseudomonas* specialized

541 metabolites. Co-culture assays and cryo-SEM imaging (Figure 6) showed that HCN and a
542 tensin-like CLP produced by Ps619 arrest the formation of streptomycete aerial hyphae and
543 subsequent sporulation, providing the pseudomonad with a competitive advantage at the
544 microbial interface.
545
546 *In planta* experiments confirmed that Ps619 could suppress potato scab and that CLP
547 production was a key determinant of this inhibitory effect (Figure 7). In contrast, HCN production
548 was not a requirement for potato scab suppression by Ps619. It is possible that HCN is not
549 produced in sufficient amounts during root colonisation for *S. scabies* inhibition, or that it instead
550 has an alternative natural role, such as metal chelation (96). The roles of the CLPs are
551 reminiscent of the interaction between *B. subtilis* and *S. coelicolor*, where the CLP surfactin
552 functions as a surfactant required for the formation of aerial structures in *B. subtilis* and arrests
553 aerial development in *S. coelicolor* (63). Collectively, these results are surprising given that
554 streptomycetes themselves use surfactants to assist in the erection of aerial mycelia (97, 98)
555 and points to secondary antagonistic roles for these molecules beyond the reduction of surface
556 tension. This is strongly supported by the inhibitory effect of purified viscosin I towards *S.*
557 *scabies* (Figure 5C).
558
559 HCN and CLPs have also been associated with insect (27) and nematode (76) killing, as well
560 as the suppression of pathogenic fungi (26, 99). This indicates that a subset of pseudomonads
561 are generalist suppressors of pathogens (and presumably also non-pathogenic organisms) due
562 to the production of these broad range antimicrobials. Genetic analysis indicates that these
563 strains are more likely to produce multiple suppressive metabolites and proteins. Evidence for
564 this is provided by the inhibition of both *P. infestans* and *G. graminis* by Ps619 Δ*hcn*Δ*ten* (Figure
565 S35). A study of the inhibitory properties of bacteria associated with the *Arabidopsis* leaf
566 microbiome showed that a large proportion of the total inhibitory activity was due to
567 *Pseudomonadales* bacteria and that a subset of individual strains were active against a wide
568 array of bacteria (100).

569

570 Unexpectedly, irrigation led to a decrease in the proportion of suppressive pseudomonads on
571 potato roots (Figure 8A) even though irrigation is one of the most effective ways to suppress
572 potato scab. One possible reason for this discrepancy is that irrigation enables non-suppressive
573 *Pseudomonas* spp. with low motility to be transported to plant roots more effectively.
574 Recruitment of non-suppressive pseudomonads to the rhizosphere may benefit the plant in
575 other ways, such as immune system priming (101, 102) or modulation of auxin biosynthesis.
576 For example, Cheng *et al.* (8) showed that auxin biosynthesis was linked to plant growth
577 promotion and induced systemic resistance by *P. fluorescens* Pf.SS101. An alternative
578 hypothesis is that changes in the overall relative abundance of soil *Pseudomonas* over
579 *Streptomyces* resulting from irrigation may override the observed shift towards less-suppressive
580 *Pseudomonas* genotypes. In support of this, drought-induced enrichment for commensal
581 *Streptomyces* and depletion of *Proteobacteria* in sorghum and rice plants have been shown to
582 be reversed by irrigation (103, 104). In this model, irrigation may reduce the relative fitness of
583 *S. scabies* versus *Pseudomonas* spp., while the microbiome of irrigated roots simultaneously
584 becomes less optimal for disease suppression.

585

586 Our data show that Ps619 is highly effective at inhibiting potato scab, yet Ps619-like strains are
587 naturally less abundant in irrigated conditions. Therefore, possible future efforts to control potato
588 scab could combine irrigation with pre-treatment with effective biocontrol strains, like Ps619, to
589 ensure tubers are colonized by a significant proportion of biocontrol strains. Such a strategy
590 could reduce the quantity of water required for effective scab suppression. While our study was
591 focused on fluorescent pseudomonads, interactions between these bacteria and the wider
592 microbiome (Figure 1) may also have a key role in potato scab suppression.

593

594 Moving forward, systematic analyses of individual organisms within microbiomes will continue
595 to help answer questions relating to microbial communities and host interactions that are difficult
596 to address using global ‘omics approaches alone. For example, the role of many bacterial

597 specialized metabolites in nature is poorly understood, especially for prolific producers such as
598 the pseudomonads and the streptomycetes (105). Future studies could examine whether the
599 host selects for bacterial populations enriched in specific BGCs and whether environmental
600 stimuli modulate the abundance of these BGCs. Synthetic microbial communities based on well-
601 characterized natural communities could then be used to test hypotheses on the role of
602 specialized metabolites in shaping the community or modulating the health of the host organism.
603

604 ## Materials and Methods

605

606 **Strains and growth conditions**

607 All strains used in this study are listed in Table S1. Unless otherwise stated, chemicals were
608 purchased from Sigma-Aldrich, enzymes from New England Biolabs, and molecular biology kits
609 from GE Healthcare and Promega. All *P. fluorescens* strains were grown at 28 °C in L medium
610 (Luria base broth, Formedium) and *Escherichia coli* at 37 °C in lysogeny broth (LB) (106). 1.3%
611 agar was added for solid media. Gentamicin was used at 25 µg/mL, carbenicillin at 100 µg/mL
612 and tetracycline (Tet) at 12.5 µg/mL. *S. scabies* spore suspensions were prepared using
613 established procedures (107).

614

615 **Soil sample collection**

616 Soil samples were collected from potato fields at RG Abrey Farms (East Wretham, Norfolk,
617 U.K., 52.4644° N, 0.8299° E). The first sampling was conducted in 2015 from two adjacent plots
618 in a single field. Soil samples were taken on 22nd January 2015, immediately prior to planting.
619 One plot was then covered loosely in polythene to protect it from irrigation. The same field sites
620 were sampled again in May at the point of maximum scab impact, once potato tubers had begun
621 to form. In this case soil samples were taken from the base of the plants, near the root system.
622 For each sampling event, a total of 12 samples were taken from three parallel potato beds at
623 regularly spaced intervals approximately one metre apart. For the second experiment, 12

624 irrigated and 12 non-irrigated potato plants were uprooted from field sites in June 2017 and
625 returned to the laboratory in large pots. Bulk soil samples were taken from these pots alongside
626 an equivalent number of rhizosphere-associated samples, which were defined as isolated root
627 systems gently shaken to remove bulk soil before processing as below. Samples were collected
628 in sterile 50 mL tubes and stored at 4 °C.
629

630 **Isolation of soil *Pseudomonas***

631 Sample processing was conducted at 4 °C throughout. 10 mL of sterile phosphate-buffered
632 saline (PBS, per litre: 8 g NaCl, 0.2 g KCl, 1.44 g Na_2HPO_4, 0.24 g KH_2PO_4, pH 7.4) were added
633 to 50 mL tubes containing 20 g of soil or root material, and vortexed vigorously for 10 minutes.
634 Samples were then filtered through a sterile muslin filter to remove larger debris. The resulting
635 suspension of soil and organic matter was centrifuged at 1000 rpm for 30 s to pellet remaining
636 soil particles, before serial dilution in PBS and plating on *Pseudomonas* selective agar. The
637 selection media comprised *Pseudomonas* agar base (Oxoid, UK) supplemented with CFC
638 (cetrimide/fucidin/cephalosporin) *Pseudomonas* selective supplement (Oxoid, UK). Plates were
639 incubated at 28 °C until colonies arose, then isolated single colonies were patched on fresh
640 CFC agar and incubated overnight at 28 °C before streaking to single colonies on King's B (KB)
641 agar plates (108). Six isolates were selected at random per soil sample and subjected to
642 phenotypic/genomic analysis.
643

644 **Amplicon sequencing**

645 Genomic DNA was isolated from 3 g of pooled soil samples using the FastDNA™ SPIN Kit for
646 soil (MP Biomedicals, UK) following the manufacturer's instructions. Genomic DNA
647 concentration and purity was determined by NanoDrop spectrophotometry as above. Microbial
648 16S rRNA genes were amplified from soil DNA samples with barcoded universal prokaryotic
649 primers (F515/R806) targeting the V4 region(109), and then subjected to Illumina® MiSeq
650 sequencing (600-cycle, 2x300 bp) at the DNA Sequencing Facility, Department of Biochemistry,

651 University of Cambridge (UK). The data was analysed using the MiSeq Reporter Metagenomics
652 Workflow (Illumina, UK) to acquire read counts for all taxonomic ranks from phylum to genus.
653 MiSeq data were visualized and analysed using Degust 3.1.0 (http://degust.erc.monash.edu/)
654 and Pheatmap (https://CRAN.R-project.org/package=pheatmap) in R 3.5.1.
655
656 **Phenotypic assays**
657 All phenotyping assays were conducted at least twice independently, and where disagreements
658 were recorded in the ordinal data, additional repeats were conducted until a firm consensus was
659 reached.
660 *Swarming motility:* 0.5% KB agar plates were poured and allowed to set and dry for 1 hour in a
661 sterile flow chamber. Plates were then inoculated with 2 µL spots of overnight cultures and
662 incubated overnight at room temperature. The motility of each isolate was tested in triplicate
663 and scored from 0 (no motility) to 3 (high motility).
664 *Secreted protease activity:* 5 µL of overnight cultures were spotted onto KB plates containing
665 1.0% skimmed milk powder. Plates were incubated at 28 °C and photographed after 24 hours,
666 with individual isolates scored as protease positive (score = 2) or negative (score = 0).
667 *Hydrogen cyanide (HCN) production:* An adaptation of the method described in Castric *et al.*
668 (110) was used. *Pseudomonas* isolates were inoculated into 150 µL of liquid KB medium in
669 individual wells of a flat bottomed 96-well plate. The plates were then overlaid with Feigl-Anger
670 reagent paper (79), prepared as follows. Whatman 3MM chromatography paper was soaked in
671 Feigl-Anger detection reagent (5 mg/mL copper(II) ethyl acetoacetate and 5 mg/mL 4,4'-
672 methylenebis(N,N-dimethylaniline) dissolved in chloroform). After complete solvent
673 evaporation, the paper was placed under the plate lid and strains were grown at 28 °C overnight
674 with gentle shaking. The intensity of blue staining on the paper was then scored from 0 (no
675 colour) to 3 (high blue intensity). The same method was applied to isolates growing on agar
676 medium.

677 *S. scabies inhibition:* Two parallel lines of *S. scabies* 87-22 spores were streaked onto SFM
678 plates (107) using a sterile toothpick. These lines were then cross streaked with overnight
679 cultures of *Pseudomonas* isolates. Plates were incubated at 30 °C and the relative performance
680 of each species was assessed daily for 5 days.
681 *P. infestans inhibition:* Assays were conducted with *P. infestans* #2006-3920A (6-A1) (The
682 Sainsbury Laboratory, UK). This was maintained on rye agar medium supplemented with 2%
683 sucrose (C-RSA) (111) at 21 °C. C-RSA was filtered through muslin fabric to enable clearer
684 observation of oomycete growth. Three 10 µL drops of overnight cultures per *Pseudomonas*
685 isolate strain were placed equidistantly 15 mm from the edge of C-RSA plates. A 3 mm plug
686 from the leading edge of a *P. infestans* culture was then placed in the centre of each plate and
687 incubated for a further 7 days at 21 °C before scoring and imaging.
688 *Take-all inhibition:* Assays were conducted with *Gaeumannomyces graminis var. tritici* strain
689 NZ.66.12 (*Ggt*) (17). Three 10 µL drops of overnight *Pseudomonas* cultures per strain were
690 placed equidistantly 15 mm from the edge of potato dextrose agar (PDA) plates and incubated
691 for 24 hours at 28 °C. *Ggt* NZ.66.12 was cultured on PDA agar for five days at room
692 temperature. A 3 mm plug from the leading edge of the NZ.66.12 culture was then placed in the
693 centre of each plate and incubated for a further five days at 22 °C before the extent of *Ggt*
694 inhibition was assessed.
695
696 **DNA extraction and Illumina® genome sequencing**
697 Single colonies of each isolate to be sequenced were picked from L agar plates and grown
698 overnight in L medium. DNA was then extracted from 2 mL of cell culture using a GenElute™
699 Bacterial Genomic DNA Kit (Sigma-Aldrich, USA). DNA samples were subjected to an initial
700 quality check using a Nanodrop spectrophotometer (Thermo Scientific, Wilmington, DE, USA)
701 before submission for Nextera library preparation and paired-end read sequencing on the
702 Illumina® MiSeq platform (600-cycle, 2x300 bp) at the DNA Sequencing Facility, Department of
703 Biochemistry, University of Cambridge (UK). Reads from 35 pseudomonads collected in

704 February 2015 were assembled into genomes using MaSuRCA v3.2.6 (112) with the following
705 settings:
706 GRAPH_KMER_SIZE=auto; USE_LINKING_MATES=1; LIMIT_JUMP_COVERAGE=60;
707 CA_PARAMETERS = ovlMerSize=30 cgwErrorRate=0.25 ovlMemory=4GB;
708 NUM_THREADS=16; JF_SIZE=100000000; DO_HOMOPOLYMER_TRIM=0.
709 Reads from 32 samples collected in May 2015 were assembled into genomes using SPAdes
710 v3.6.2 (113) with k-mer flag set to -k 21,33,55,77,99,127. All assembly tasks were conducted
711 using 16 CPUs on a 256 GB compute node within the Norwich Bioscience Institutes (NBI) High
712 Performance Computing cluster. An additional strain from May 2015 (Ps925) was sequenced
713 and assembled by MicrobesNG (http://www.microbesng.uk), which is supported by the BBSRC
714 (grant number BB/L024209/1). The 69 assembled genome sequences were annotated using
715 Prokka (114), which implements Prodigal (115) as an open reading frame calling tool. Assembly
716 qualities were assessed using CheckM (116). Genome assemblies are available at the
717 European Nucleotide Archive (http://www.ebi.ac.uk/ena/) with the project accession
718 PRJEB34261.
719
720 **Phylogenetic and bioinformatic analysis**
721 The *gyrB* housekeeping gene sequence was identified in each newly sequenced genome by
722 BLAST comparison with the sequence of *gyrB* from *P. fluorescens* SBW25. The full-length *gyrB*
723 sequences from these strains and several reference strains were aligned using MUSCLE 3.8.31
724 (117) with default settings, then a maximum likelihood tree was calculated using RAxML 8.2.12
725 (118) on the CIPRES portal (119) with the following parameters: raxmlHPC-HYBRID-AVX -T 4
726 -f a -N autoMRE -n result -s infile.txt -c 25 -m GTRCAT -p 12345 -k -x 12345. Genomes were
727 subjected to bioinformatic analysis as described in the Supplementary Information.
728 Phylogenetic trees and presence/absence data for accessory genes were visualised using
729 Interactive Tree of Life (iTOL) (120), with *Pseudomonas aeruginosa* PAO1 *gyrB* as the
730 outgroup.

731

732 **Molecular biology procedures**

733 Cloning was carried out in accordance with standard molecular biology techniques. *P.*
734 *fluorescens* deletion mutants were constructed by allelic exchange as described previously
735 (121). Up- and downstream flanking regions (approx. 500 bp) to the target genes were amplified
736 using primers listed in Table S2. PCR products in each case were ligated into pTS1 (122)
737 between XhoI and BamHI. The resulting deletion vectors were transformed into the target
738 strains by electroporation, and single crossovers selected on L + Tet and re-streaked to isolate
739 single colonies. 100 mL cultures in L medium from single crossovers were grown overnight at
740 28 °C, then plated onto L + 10% sucrose plates to counter-select for double crossovers.
741 Individual colonies from these plates were then patched onto L plates ± Tet, with Tet-sensitive
742 colonies tested for gene deletion by colony PCR using primers external to the deleted gene in
743 each case (Table S2).

744

745 Luminescent-tagged strains were produced by introduction of the *Aliivibrio fischeri luxCDABE*
746 cassette into the neutral *att::Tn7* site in *Pseudomonas* chromosomes using the Tn7-based
747 expression system described in Choi *et al.* (74). Strains were electroporated with plasmids
748 pUC18-mini*Tn7*T-Gm-*lux* and the helper pTNS2, and transformant colonies were grown on solid
749 L medium + gentamicin for 2-3 days at 28 °C. Integration of the *lux* cassette into *Pseudomonas*
750 genomes was confirmed by PCR and with a luminometer. Luminescent cells were then tracked
751 using the NightOWL visualisation system (Berthold Technologies, Germany). All plasmids used
752 in this study are reported in Table S3.

753

754 **Liquid chromatography - mass spectrometry detection of lipopeptides**

755 *Pseudomonas* isolates were grown overnight in L medium (10 mL) for 16 hours at 28 °C. 100
756 µL of each culture was used to inoculate 40 mm diameter KB agar plates. Plates were incubated
757 for 24 hours at 28 °C, before the agar from each plate was decanted into a sterile 50 mL tube

758 and extracted with 10 mL 50% EtOH with occasional vortexing for 3 hours. 2 mL was taken from
759 each sample and centrifuged in 2 mL tubes for 5 min at 16,000 g. The supernatant was collected
760 and stored at -80 °C. Samples were diluted with an equal volume of water, then subjected to
761 LC-MS analysis using a Shimadzu Nexera X2 UHPLC coupled to a Shimadzu ion-trap time-of-
762 flight (IT-TOF) mass spectrometer. Samples (5 µL) were injected onto a Phenomenex Kinetex
763 2.6 µm XB-C18 column (50 x 2.1mm, 100 Å), eluting with a linear gradient of 5 to 95%
764 acetonitrile in water + 0.1% formic acid over 6 minutes with a flow-rate of 0.6 mL/min at 40 °C.
765 To compare the retention times of viscosin I (Ps682), WLIP (*Pseudomonas* sp. LMG 2338) and
766 viscosin (*P. fluorescens* SBW25), extracts were prepared from their producing organisms as
767 described above. The same chromatography conditions as above were used, but with a linear
768 gradient of 5 to 100% acetonitrile in water + 0.1% formic acid over 15 minutes.
769
770 Positive mode mass spectrometry data was collected between *m/z* 300 and 2000 with an ion
771 accumulation time of 10 ms featuring an automatic sensitivity control of 70% of the base peak.
772 The curved desolvation line temperature was 300 °C and the heat block temperature was 250
773 °C. MS/MS data was collected in a data-dependent manner using collision-induced dissociation
774 energy of 50% and a precursor ion width of 3 Da. The instrument was calibrated using sodium
775 trifluoroacetate cluster ions prior to every run.
776
777 A molecular network was created using the online workflow at the Global Natural Product Social
778 Molecular Networking (GNPS) site (https://gnps.ucsd.edu/) (72). The data was filtered by
779 removing all MS/MS peaks within +/- 17 Da of the precursor *m/z*. The data was then clustered
780 with MS-Cluster with a parent mass tolerance of 1 Da and a MS/MS fragment ion tolerance of
781 0.5 Da to create consensus spectra. Consensus spectra that contained less than 2 spectra were
782 discarded. A network was then created where edges were filtered to have a cosine score above
783 0.6 and more than 4 matched peaks. Further edges between two nodes were kept in the network
784 if each of the nodes appeared in each other's respective top 10 most similar nodes. The spectra

785 in the network were then searched against GNPS spectral libraries. The library spectra were
786 filtered in the same manner as the input data. All matches kept between network spectra and
787 library spectra were required to have a score above 0.7 and at least 4 matched peaks. Networks
788 were visualised using Cytoscape v3.8.2 (123) and the data was manually filtered to remove
789 duplicate nodes (same *m/z* and retention time). The data is available as a MassIVE dataset at
790 ftp://massive.ucsd.edu/MSV000084283/ and the GNPS analysis is available here:
791 https://gnps.ucsd.edu/ProteoSAFe/status.jsp?task=51ac5fe596424cf88cfc17898985cac2
792
793 High-resolution mass spectra were acquired on a Synapt G2-Si mass spectrometer equipped
794 with an Acquity UPLC (Waters). Aliquots of the samples were injected onto an Acquity UPLC®
795 BEH C18 column, 1.7 µm, 1x100 mm (Waters) and eluted with a gradient of acetonitrile/0.1%
796 formic acid (B) in water/0.1% formic acid (A) with a flow rate of 0.08 mL/min at 45 °C. The
797 concentration of B was kept at 1% for 1 min followed by a gradient up to 40% B in 9 min, ramping
798 to 99% B in 1 min, kept at 99% B for 2 min and re-equilibrated at 1% B for 4 min. MS data were
799 collected in positive mode with the following parameters: resolution mode, positive ion mode,
800 scan time 0.5 s, mass range *m/z* 50-1200 calibrated with sodium formate, capillary voltage =
801 2.5 kV; cone voltage = 40 V; source temperature = 125 °C; desolvation temperature = 300 °C.
802 Leu-enkephalin peptide was used to generate a lock-mass calibration with 556.2766, measured
803 every 30 s during the run. For MS/MS fragmentation, a data directed analysis (DDA) method
804 was used with the following parameters: precursor selected from the 4 most intense ions; MS2
805 threshold: 5,000; scan time 0.5 s; no dynamic exclusion. In positive mode, collision energy (CE)
806 was ramped between 10-30 at low mass (*m/z* 50) and 15-60 at high mass (*m/z* 1200).
807
808 **Purification and characterisation of viscosin I**
809 Pre-cultures of Ps682 were grown in 10 mL LB medium for 16 hours and 600 µL aliquots were
810 used to inoculate 140 mm diameter KB agar plates. Fifteen plates were inoculated and
811 incubated for 24 hours. The agar was decanted and extracted with 500 mL ethyl acetate for 2

812 hours with occasional mixing. The organic fraction was filtered off, washed with 3 x 200 mL
813 water, dried over $MgSO_4$, and then solvent was removed *in vacuo*. The resulting material was
814 dissolved in MeOH and applied to a 12 g C18 flash chromatography column (Biotage), pre-
815 equilibrated in 70% MeOH. Separation proceeded by a gradient of 70-100% MeOH over 10
816 column volumes. Each fraction was subject to LC-MS analysis using a Shimadzu Nexera X2
817 UHPLC coupled to a Shimadzu IT-TOF mass spectrometer, as described above.
818
819 Solvent was removed from viscosin I-containing fractions using a rotary evaporator and then a
820 Genevac (SP Scientific). Fractions were then dissolved in MeOH to 1 mg/mL and further purified
821 using a Thermo Dionex Ultimate 3000 HPLC system. 200 µL aliquots were injected onto a
822 Phenomenex C18 Luna column (5 µm, 250 mm x 10 mm) and eluted with a linear gradient of
823 5% to 95% acetonitrile/H_2O over 30 minutes, with a flow rate of 4 mL/min and UV absorption
824 data collected at 210 nm. LC-MS analysis (as described above) was used to identify pure
825 fractions, which were combined and dried *in vacuo* to yield 1.4 mg viscosin I as a white powder.
826
827 Viscosin I (1.4 mg) was dissolved in *N,N*-dimethylformamide-d_7 (DMF-d_7) and nuclear magnetic
828 resonance (NMR) spectra were acquired on a Bruker Avance Neo 600 MHz spectrometer
829 equipped with a TCI cryoprobe. The experiments were carried out at 298 K with the residual
830 DMF solvent used as an internal standard (δ_H/δ_C 2.75/29.76). The residual solvent signal from
831 H_2O was suppressed through a presaturation sequence in 1D ^1H. Resonances were assigned
832 through 1D ^1H and DEPT135 experiments, and 2D COSY, HSQCed, HMBC, TOCSY and
833 HSQC-TOCSY experiments. Spectra were analysed using Bruker TopSpin 3.5 and Mestrelab
834 Research Mnova 14.0 software. NMR data are reported in Figures S19-S29 and Table S4.
835
836 **Disk Diffusion Assays**
837 A *S. scabies* 87-22 spore suspension was diluted 1:100 in sterile MQ water and 60 µL aliquots
838 were applied to instant potato medium (20 g/L Smash™ Instant Mash, 20 g/L agar) on 100 mm

839 square plates. The spore solution was evenly distributed using a sterile cotton bud and the plate
840 was dried for 30 min. Viscosin I was diluted in MeOH to produce a range of concentrations from
841 20 to 100 µg/mL. Each concentration was applied to a 6 mm filter paper disk, in 5 x 20 µL
842 applications at 10 min intervals, and then dried for 30 min. The disks were then applied to the
843 surface of the agar plate, which was incubated at 30 °C and imaged daily.
844
845 **Scanning electron microscopy**
846 Small pieces of the *Pseudomonas-Streptomyces* co-culture samples were excised from the
847 surface of agar plates and mounted on an aluminium stub using Tissue Tek^{R} (BDH Laboratory
848 Supplies, Poole, England). The stub was then immediately plunged into liquid nitrogen slush at
849 approximately -210 °C to cryo-preserve the material. The sample was transferred onto the
850 cryostage of an ALTO 2500 cryo-transfer system (Gatan, Oxford, England) attached to an FEI
851 Nova NanoSEM 450 (FEI, Eindhoven, The Netherlands). Sublimation of surface frost was
852 performed at -95 °C for three minutes before sputter coating the sample with platinum for 3 min
853 at 10 mA, at colder than -110 °C. After sputter-coating, the sample was moved onto the cryo-
854 stage in the main chamber of the microscope, held at -125 °C. The sample was imaged at 3 kV
855 and digital TIFF files were stored.
856
857 **Potato scab biocontrol assays**
858 *In planta* assays were performed as described previously (124, 125) with some modifications.
859 Briefly, 2 L of GYM (4 g/L glucose, 4 g/L yeast extract, 10 g/L malt extract, 2 g/L $CaCO_3$, pH
860 7.2) was inoculated with a *S. scabies* 87-22 starter culture from a spore suspension and
861 incubated for 48 h at 30 °C, 250 rpm. Each culture was then centrifuge at 16,994 x *g* for 15 min
862 and washed twice with PBS (2 L). *Pseudomonas* strains Ps619, Ps682 and associated mutants
863 were grown overnight at 28 °C, 250 rpm in 50 mL L medium (Luria base broth, Formedium),
864 centrifuged at 1,520 x *g* for 15 min, washed twice with PBS (20 mL) and adjusted to OD600 =
865 0.2 for the final inoculation.

866

867 50 mL of autoclaved vermiculite and 50 mL of bacterial culture were mixed to constitute the final
868 inoculum. 5 L pots were filled with steam-sterilised substrate (John Innes Cereal Mix) and
869 inoculum was applied into the pots and mixed with the soil. Different combinations of bacterial
870 inocula were made accordingly following the same method. Potato seeds cv. Maris Piper
871 obtained from VCS Potatoes Ltd (Suffolk, UK) were surfaced disinfected by immersion in 1%
872 sodium hypochlorite for 15 min. Tubers were then rinsed with water, air-dried and placed in
873 pots. Pots were watered until saturation according to their growth stage. Potato plants were
874 grown in a glasshouse with a light cycle of 16h/8h at 18-20 °C. Two independent experiments
875 were run between 17th July - 6th November 2020 and 31st July - 20th November 2020, and three
876 - four plants were used per treatment. Tubers were collected, washed, weighed and scored
877 accordingly to a one to six scale as described in Andrade *et al*. (81). Potato plants were dried
878 for four days at 30 °C and aerial parts and tuber weights were both recorded, as well as tuber
879 number. Treatment differences were carried out based on the disease index (DI) of each plant
880 (n=4 for each treatment). The DI was calculated as the mean of all the scored tubers per plant
881 and *p* values were calculated using Dunnett's multiple comparison test.

882

883 **Acknowledgements**

884 Financial support was provided by a Royal Society University Research Fellowship to Andrew
885 Truman, Biotechnology and Biological Sciences Research Council (BBSRC) BIO, MET, PH and
886 MfN Institute Strategic Programme grants to the John Innes Centre (JIC), a JIC Institute
887 Development Grant and NPRONET Proof of Concept grant. Jonathan Ford was supported by
888 a BBSRC DTP studentship and Alba Pacheco-Moreno was supported by a BBSRC iCASE PhD
889 studentship, both awarded to the Norwich Research Park. We thank Prof. Jonathan Jones (The
890 Sainsbury Laboratory) for providing *P. infestans* isolates and Dr Tim Mauchline (Rothamsted
891 Research) for providing *Ggt* NZ.66.12. We thank the JIC Bioimaging, Metabolomics and NMR
892 facilities for their contribution to this publication, Dr Carlo de Oliveira Martins (JIC) for assistance

with mass spectrometry, and Dr Natalia Miguel-Vior (JIC) for assistance with potato scab biocontrol assays.

References

1. Larkin, R. P., Honeycutt, C. W., Griffin, T. S., Olanya, O. M., Halloran, J. M. and He, Z. (2011) Effects of different potato cropping system approaches and water management on soilborne diseases and soil microbial communities. *Phytopathology* **101**, 58–67. DOI: 10.1094/PHYTO-04-10-0100.
2. Lerat, S., Simao-Beaunoir, A.-M. snd Beaulieu, C. (2009) Genetic and physiological determinants of *Streptomyces scabies* pathogenicity. *Molecular Plant Pathology* **10**, 579–585. DOI: 10.1111/j.1364-3703.2009.00561.x.
3. Bignell, D. R. D., Huguet-Tapia, J. C., Joshi, M. V., Pettis, G. S. and Loria, R. (2010) What does it take to be a plant pathogen: genomic insights from *Streptomyces* species. *Antonie van Leeuwenhoek* **98**, 179–194. DOI: 10.1007/s10482-010-9429-1.
4. Weller, D. M. (2007) *Pseudomonas* biocontrol agents of soilborne pathogens: looking back over 30 years. *Phytopathology* **97**, 250–256. DOI: 10.1094/PHYTO-97-2-0250.
5. Köhl, J., Kolnaar, R. and Ravensberg, W. J. (2019) Mode of Action of Microbial Biological Control Agents Against Plant Diseases: Relevance Beyond Efficacy. *Front Plant Sci* **10**. DOI: 10.3389/fpls.2019.00845.
6. Loper, J. E., Hassan, K. A., Mavrodi, D. V., Davis, E. W., Lim, C. K., Shaffer, B. T., Elbourne, L. D. H., Stockwell, V. O., Hartney, S. L., Breakwell, K., Henkels, M. D., Tetu, S. G., Rangel, L. I., Kidarsa, T. A., Wilson, N. L., van de Mortel, J. E., Song, C., Blumhagen, R., Radune, D., Hostetler, J. B., Brinkac, L. M., Durkin, A. S., Kluepfel, D. A., Wechter, W. P., Anderson, A. J., Kim, Y. C., Pierson, L. S., Pierson, E. A., Lindow, S. E., Kobayashi, D. Y., Raaijmakers, J. M., Weller, D. M., Thomashow, L. S., Allen, A. E. and Paulsen, I. T. (2012) Comparative Genomics of Plant-Associated *Pseudomonas* spp.: Insights into Diversity and Inheritance of Traits Involved in Multitrophic Interactions. *PLoS Genet* **8**, e1002784. DOI: 10.1371/journal.pgen.1002784.s027.

921 7. Zamioudis, C., Mastranesti, P., Dhonukshe, P., Blilou, I. and Pieterse, C. M. J. (2013)
922 Unraveling Root Developmental Programs Initiated by Beneficial *Pseudomonas* spp.
923 Bacteria. *Plant Physiol.* **162**, 304–318. DOI: 10.1104/pp.112.212597.
924 8. Cheng, X., Etalo, D. W., van de Mortel, J. E., Dekkers, E., Nguyen, L., Medema, M. H.
925 and Raaijmakers, J. M. (2017) Genome-wide analysis of bacterial determinants of plant
926 growth promotion and induced systemic resistance by *Pseudomonas fluorescens*.
927 *Environmental Microbiology* **19**, 4638–4656. DOI: 10.1111/1462-2920.13927.
928 9. Haas, D. and Défago, G. (2005) Biological control of soil-borne pathogens by
929 fluorescent pseudomonads. *Nat Rev Micro* **3**, 307–319. DOI: 10.1038/nrmicro1129.
930 10. Biessy, A., Novinscak, A., Blom, J., Léger, G., Thomashow, L. S., Cazorla, F. M., Josic,
931 D. and Filion, M. (2019) Diversity of phytobeneficial traits revealed by whole-genome
932 analysis of worldwide-isolated phenazine-producing *Pseudomonas* spp. *Environmental*
933 *Microbiology* **21**, 437–455. DOI: 10.1111/1462-2920.14476.
934 11. Gross, H. and Loper, J. E. (2009) Genomics of secondary metabolite production by
935 *Pseudomonas* spp. *Nat. Prod. Rep.* **26**, 1408–1446. DOI: 10.1039/b817075b.
936 12. Nguyen, D. D., Melnik, A. V., Koyama, N., Lu, X., Schorn, M., Fang, J., Aguinaldo, K.,
937 Lincecum, T. L., Jr, Ghequire, M. G. K., Carrión, V. J., Cheng, T. L., Duggan, B. M.,
938 Malone, J. G., Mauchline, T. H., Sanchez, L. M., Kilpatrick, A. M., Raaijmakers, J. M.,
939 De Mot, R., Moore, B. S., Medema, M. H. and Dorrestein, P. C. (2016) Indexing the
940 *Pseudomonas* specialized metabolome enabled the discovery of poaeamide B and the
941 bananamides. *Nature Microbiology* **2**, 1–9. DOI: 10.1038/nmicrobiol.2016.197.
942 13. Stringlis, I. A., Zhang, H., Pieterse, C. M. J., Bolton, M. D. and de Jonge, R. (2018)
943 Microbial small molecules - weapons of plant subversion. *Nat. Prod. Rep.* **35**, 410–433.
944 DOI: 10.1039/c7np00062f.
945 14. Arseneault, T., Goyer, C. and Filion, M. (2013) Phenazine Production by *Pseudomonas*
946 sp. LBUM223 Contributes to the Biological Control of Potato Common Scab.
947 *Phytopathology* **103**, 995–1000. DOI: 10.1094/PHYTO-01-13-0022-R.

948 15. Ghequire, M. G. K. and De Mot, R. (2014) Ribosomally encoded antibacterial proteins
949 and peptides from *Pseudomonas*. *FEMS Microbiol Rev* **38**, 523–568. DOI:
950 10.1111/1574-6976.12079.
951 16. Rangel, L. I., Henkels, M. D., Shaffer, B. T., Walker, F. L., Davis, E. W., Stockwell, V. O.,
952 Bruck, D., Taylor, B. J. and Loper, J. E. (2016) Characterization of Toxin Complex Gene
953 Clusters and Insect Toxicity of Bacteria Representing Four Subgroups of *Pseudomonas*
954 *fluorescens*. *PLoS ONE* **11**, e0161120. DOI: 10.1371/journal.pone.0161120.
955 17. Mauchline, T. H., Chedom-Fotso, D., Chandra, G., Samuels, T., Greenaway, N.,
956 Backhaus, A., McMillan, V., Canning, G., Powers, S. J., Hammond-Kosack, K. E.,
957 Hirsch, P. R., Clark, I. M., Mehrabi, Z., Roworth, J., Burnell, J. and Malone, J. G. (2015)
958 An analysis of *Pseudomonas* genomic diversity in take-all infected wheat fields reveals
959 the lasting impact of wheat cultivars on the soil microbiota. *Environmental Microbiology*
960 **17**, 4764–4778. DOI: 10.1111/1462-2920.13038.
961 18. Wei, Z., Gu, Y., Friman, V.-P., Kowalchuk, G. A., Xu, Y., Shen, Q. and Jousset, A.
962 (2019) Initial soil microbiome composition and functioning predetermine future plant
963 health. *Sci Adv* **5**, eaaw0759. DOI: 10.1126/sciadv.aaw0759.
964 19. Kwak, Y.-S. and Weller, D. M. (2013) Take-all of Wheat and Natural Disease
965 Suppression: A Review. *Plant Pathol. J.* **29**, 125–135. DOI:
966 10.5423/PPJ.SI.07.2012.0112.
967 20. Silby, M. W., Cerdeño-Tárraga, A. M., Vernikos, G. S., Giddens, S. R., Jackson, R. W.,
968 Preston, G. M., Zhang, X.-X., Moon, C. D., Gehrig, S. M., Godfrey, S. A. C., Knight, C.
969 G., Malone, J. G., Robinson, Z., Spiers, A. J., Harris, S., Challis, G. L., Yaxley, A. M.,
970 Harris, D., Seeger, K., Murphy, L., Rutter, S., Squares, R., Quail, M. A., Saunders, E.,
971 Mavromatis, K., Brettin, T. S., Bentley, S. D., Hothersall, J., Stephens, E., Thomas, C.
972 M., Parkhill, J., Levy, S. B., Rainey, P. B. and Thomson, N. R. (2009) Genomic and
973 genetic analyses of diversity and plant interactions of *Pseudomonas fluorescens*.
974 *Genome Biol.* **10**, R51. DOI: 10.1186/gb-2009-10-5-r51.

975 21. Gomila, M., Peña, A., Mulet, M., Lalucat, J. and García-Valdés, E. (2015)
976 Phylogenomics and systematics in *Pseudomonas*. *Front. Microbiol.* **6**, 214. DOI:
977 10.3389/fmicb.2015.00214.
978 22. Melnyk, R. A., Hossain, S. S. and Haney, C. H. (2019) Convergent gain and loss of
979 genomic islands drive lifestyle changes in plant-associated *Pseudomonas*. *ISME J.* **13**,
980 1575–1588. DOI: 10.1038/s41396-019-0372-5.
981 23. Garrido-Sanz, D., Meier-Kolthoff, J. P., Göker, M., Martín, M., Rivilla, R. and Redondo-
982 Nieto, M. (2016) Genomic and Genetic Diversity within the *Pseudomonas fluorescens*
983 Complex. *PLoS ONE* **11**, e0150183. DOI: 10.1371/journal.pone.0150183.
984 24. Little, R. H., Woodcock, S. D., Campilongo, R., Fung, R. K. Y., Heal, R., Humphries, L.,
985 Pacheco-Moreno, A., Paulusch, S., Stigliano, E., Vikeli, E., Ward, D. and Malone, J. G.
986 (2019) Differential Regulation of Genes for Cyclic-di-GMP Metabolism Orchestrates
987 Adaptive Changes During Rhizosphere Colonization by *Pseudomonas fluorescens*.
988 *Front. Microbiol.* **10**, 1089. DOI: 10.3389/fmicb.2019.01089.
989 25. Arseneault, T., Goyer, C. and Filion, M. (2015) *Pseudomonas fluorescens* LBUM223
990 Increases Potato Yield and Reduces Common Scab Symptoms in the Field.
991 *Phytopathology* **105**, 1311–1317. DOI: 10.1094/PHYTO-12-14-0358-R.
992 26. Michelsen, C. F., Watrous, J., Glaring, M. A., Kersten, R., Koyama, N., Dorrestein, P. C.
993 and Stougaard, P. (2015) Nonribosomal peptides, key biocontrol components for
994 *Pseudomonas fluorescens* In5, isolated from a Greenlandic suppressive soil. *mBio* **6**,
995 e00079. DOI: 10.1128/mBio.00079-15.
996 27. Flury, P., Vesga, P., Péchy-Tarr, M., Aellen, N., Dennert, F., Hofer, N., Kupferschmied,
997 K. P., Kupferschmied, P., Metla, Z., Ma, Z., Siegfried, S., de Weert, S., Bloemberg, G.,
998 Höfte, M., Keel, C. J. and Maurhofer, M. (2017) Antimicrobial and Insecticidal: Cyclic
999 Lipopeptides and Hydrogen Cyanide Produced by Plant-Beneficial *Pseudomonas*
1000 Strains CHA0, CMR12a, and PCL1391 Contribute to Insect Killing. *Front Microbiol* **8**,
1001 100. DOI: 10.3389/fmicb.2017.00100.

1002 28. Elphinstone, J. G., Thwaites, R., Stalham, M. and Wale, S. (2009) Integration of
1003 precision irrigation and non-water based measures to suppress common scab of potato
1004 (Potato Council Project Report). https://ahdb.org.uk/integration-of-precision-irrigation-
1005 and-non-water-based-measures-to-suppress-common-scab-of-potato [accessed June
1006 2021]
1007 29. Rosenzweig, N., Tiedje, J. M., Quensen, J. F., III, Meng, Q. and Hao, J. J. (2012)
1008 Microbial communities associated with potato common scab-suppressive soil
1009 determined by pyrosequencing analyses. *Plant Disease* **96**, 718–725. DOI:
1010 10.1094/PDIS-07-11-0571.
1011 30. Meng, Q., Yin, J., Rosenzweig, N., Douches, D. and Hao, J. J. (2012) Culture-based
1012 assessment of microbial communities in soil suppressive to potato common scab. *Plant*
1013 *disease* **96**, 712–717. DOI: 10.1094/PDIS-05-11-0441.
1014 31. Arseneault, T., Goyer, C. and Filion, M. (2016) Biocontrol of Potato Common Scab is
1015 Associated with High *Pseudomonas fluorescens* LBUM223 Populations and Phenazine-
1016 1-Carboxylic Acid Biosynthetic Transcript Accumulation in the Potato Geocaulosphere.
1017 *Phytopathology* **106**, 963–970. DOI: 10.1094/PHYTO-01-16-0019-R.
1018 32. Fierer, N. (2017) Embracing the unknown: disentangling the complexities of the soil
1019 microbiome. *Nat Rev Micro* **15**, 579–590. DOI: 10.1038/nrmicro.2017.87.
1020 33. Mauchline, T. H. and Malone, J. G. (2017) Life in earth - the root microbiome to the
1021 rescue? *Curr. Opin. Microbiol.* **37**, 23–28. DOI: 10.1016/j.mib.2017.03.005.
1022 34. Law, C. W., Chen, Y., Shi, W. and Smyth, G. K. (2014) voom: Precision weights unlock
1023 linear model analysis tools for RNA-seq read counts. *Genome Biol.* **15**, R29. DOI:
1024 10.1186/gb-2014-15-2-r29.
1025 35. Weinert, N., Piceno, Y., Ding, G.-C., Meincke, R., Heuer, H., Berg, G., Schloter, M.,
1026 Andersen, G. and Smalla, K. (2011) PhyloChip hybridization uncovered an enormous
1027 bacterial diversity in the rhizosphere of different potato cultivars: many common and few
1028 cultivar-dependent taxa. *FEMS Microbiol. Ecol.* **75**, 497–506. DOI: 10.1111/j.1574-
1029 6941.2010.01025.x.

1030 36. Pfeiffer, S., Mitter, B., Oswald, A., Schloter-Hai, B., Schloter, M., Declerck, S. and
1031 Sessitsch, A. (2017) Rhizosphere microbiomes of potato cultivated in the High Andes
1032 show stable and dynamic core microbiomes with different responses to plant
1033 development. *FEMS Microbiol. Ecol.* **93**, fiw242. DOI: 10.1093/femsec/fiw242.
1034 37. Blin, K., Shaw, S., Steinke, K., Villebro, R., Ziemert, N., Lee, S. Y., Medema, M. H. and
1035 Weber, T. (2019) antiSMASH 5.0: updates to the secondary metabolite genome mining
1036 pipeline. *Nucleic Acids Res.* **47**, W81–W87. DOI: 10.1093/nar/gkz310.
1037 38. Pessi, G. and Haas, D. (2000) Transcriptional control of the hydrogen cyanide
1038 biosynthetic genes hcnABC by the anaerobic regulator ANR and the quorum-sensing
1039 regulators LasR and RhlR in *Pseudomonas aeruginosa*. *Journal of Bacteriology* **182**,
1040 6940–6949. DOI: 10.1128/JB.182.24.6940-6949.2000.
1041 39. Metelev, M., Serebryakova, M., Ghilarov, D., Zhao, Y. and Severinov, K. (2013)
1042 Structure of microcin B-like compounds produced by *Pseudomonas syringae* and
1043 species specificity of their antibacterial action. *Journal of Bacteriology* **195**, 4129–4137.
1044 DOI: 10.1128/JB.00665-13.
1045 40. Palm, C. J., Gaffney, T. and Kosuge, T. (1989) Cotranscription of genes encoding
1046 indoleacetic acid production in *Pseudomonas syringae* subsp. *savastanoi*. *Journal of*
1047 *Bacteriology* **171**, 1002–1009. DOI: 10.1128/jb.171.2.1002-1009.1989.
1048 41. McClerklin, S. A., Lee, S. G., Harper, C. P., Nwumeh, R., Jez, J. M. and Kunkel, B. N.
1049 (2018) Indole-3-acetaldehyde dehydrogenase-dependent auxin synthesis contributes to
1050 virulence of *Pseudomonas syringae* strain DC3000. *PLoS Pathog.* **14**, e1006811. DOI:
1051 10.1371/journal.ppat.1006811.
1052 42. Medema, M. H., Takano, E. and Breitling, R. (2013) Detecting sequence homology at
1053 the gene cluster level with MultiGeneBlast. *Molecular Biology and Evolution* **30**, 1218–
1054 1223. DOI: 10.1093/molbev/mst025.
1055 43. Raaijmakers, J. M., de Bruijn, I., Nybroe, O. and Ongena, M. (2010) Natural functions of
1056 lipopeptides from *Bacillus* and *Pseudomonas*: more than surfactants and antibiotics.
1057 *FEMS Microbiol Rev* **34**, 1037–1062. DOI: 10.1111/j.1574-6976.2010.00221.x.

1058 44. Cimermancic, P., Medema, M. H., Claesen, J., Kurita, K., Wieland Brown, L. C.,
1059 Mavrommatis, K., Pati, A., Godfrey, P. A., Koehrsen, M., Clardy, J., Birren, B. W.,
1060 Takano, E., Sali, A., Linington, R. G. and Fischbach, M. A. (2014) Insights into
1061 secondary metabolism from a global analysis of prokaryotic biosynthetic gene clusters.
1062 *Cell* **158**, 412–421. DOI: 10.1016/j.cell.2014.06.034.
1063 45. Cézard, C., Farvacques, N. and Sonnet, P. (2015) Chemistry and biology of
1064 pyoverdines, *Pseudomonas* primary siderophores. *Curr. Med. Chem.* **22**, 165–186.
1065 46. Berti, A. D. and Thomas, M. G. (2009) Analysis of achromobactin biosynthesis by
1066 *Pseudomonas syringae* pv. *syringae* B728a. *Journal of Bacteriology* **191**, 4594–4604.
1067 DOI: 10.1128/JB.00457-09.
1068 47. Matthijs, S., Budzikiewicz, H., Schäfer, M., Wathelet, B. and Cornelis, P. (2008)
1069 Ornicorrugatin, a New Siderophore from *Pseudomonas fluorescens* AF76. *Zeitschrift für*
1070 *Naturforschung C* **63**, 8–12. DOI: 10.1515/znc-2008-1-202.
1071 48. Patel, H. M. and Walsh, C. T. (2001) In Vitro Reconstitution of the *Pseudomonas*
1072 *aeruginosa* Nonribosomal Peptide Synthesis of Pyochelin: Characterization of
1073 Backbone Tailoring Thiazoline Reductase and N-Methyltransferase Activities.
1074 *Biochemistry* **40**, 9023–9031. DOI: 10.1021/bi010519n.
1075 49. Mercado-Blanco, J., van der Drift, K. M., Olsson, P. E., Thomas-Oates, J. E., van Loon,
1076 L. C. and Bakker, P. A. (2001) Analysis of the pmsCEAB gene cluster involved in
1077 biosynthesis of salicylic acid and the siderophore pseudomonine in the biocontrol strain
1078 *Pseudomonas fluorescens* WCS374. *Journal of Bacteriology* **183**, 1909–1920. DOI:
1079 10.1128/JB.183.6.1909-1920.2001.
1080 50. Kim, S. Y., Ju, K.-S., Metcalf, W. W., Evans, B. S., Kuzuyama, T. and van der Donk, W.
1081 A. (2012) Different biosynthetic pathways to fosfomycin in *Pseudomonas syringae* and
1082 *Streptomyces* species. *Antimicrob. Agents Chemother.* **56**, 4175–4183. DOI:
1083 10.1128/AAC.06478-11.

1084 51. Repka, L. M., Chekan, J. R., Nair, S. K. and van der Donk, W. A. (2017) Mechanistic
1085 Understanding of Lanthipeptide Biosynthetic Enzymes. *Chem. Rev.* **117**, 5457–5520.
1086 DOI: 10.1021/acs.chemrev.6b00591.
1087 52. Velasco, A., Acebo, P., Gomez, A., Schleissner, C., Rodríguez, P., Aparicio, T., Conde,
1088 S., Muñoz, R., la Calle, de, F., Garcia, J. L. and Sánchez-Puelles, J. M. (2005)
1089 Molecular characterization of the safracin biosynthetic pathway from *Pseudomonas*
1090 *fluorescens* A2-2: designing new cytotoxic compounds. *Mol. Microbiol.* **56**, 144–154.
1091 DOI: 10.1111/j.1365-2958.2004.04433.x.
1092 53. Coulthurst, S. J., Barnard, A. M. L. and Salmond, G. P. C. (2005) Regulation and
1093 biosynthesis of carbapenem antibiotics in bacteria. *Nat. Rev. Micro.* **3**, 295–306. DOI:
1094 10.1038/nrmicro1128.
1095 54. Kudo, F. and Eguchi, T. (2009) Biosynthetic genes for aminoglycoside antibiotics. *The*
1096 *Journal of Antibiotics* **62**, 471–481. DOI: 10.1038/ja.2009.76.
1097 55. Leveau, J. H. J. and Gerards, S. (2008) Discovery of a bacterial gene cluster for
1098 catabolism of the plant hormone indole 3-acetic acid. *FEMS Microbiol. Ecol.* **65**, 238–
1099 250. DOI: 10.1111/j.1574-6941.2008.00436.x.
1100 56. Puehringer, S., Metlitzky, M. and Schwarzenbacher, R. (2008) The pyrroloquinoline
1101 quinone biosynthesis pathway revisited: a structural approach. *BMC Biochem.* **9**, 8. DOI:
1102 10.1186/1471-2091-9-8.
1103 57. Choi, O., Kim, J., Kim, J.-G., Jeong, Y., Moon, J. S., Park, C. S. and Hwang, I. (2008)
1104 Pyrroloquinoline quinone is a plant growth promotion factor produced by *Pseudomonas*
1105 *fluorescens* B16. *Plant Physiol.* **146**, 657–668. DOI: 10.1104/pp.107.112748.
1106 58. Zachow, C., Jahanshah, G., de Bruijn, I., Song, C., Ianni, F., Pataj, Z., Gerhardt, H.,
1107 Pianet, I., Lämmerhofer, M., Berg, G., Gross, H. and Raaijmakers, J. M. (2015) The
1108 Novel Lipopeptide Poaeamide of the Endophyte *Pseudomonas poae* RE*1-1-14 Is
1109 Involved in Pathogen Suppression and Root Colonization. *Mol. Plant Microbe Interact.*
1110 **28**, 800–810. DOI: 10.1094/MPMI-12-14-0406-R.

1111 59. Hunziker, L., Bönisch, D., Groenhagen, U., Bailly, A., Schulz, S. and Weisskopf, L.
1112 (2015) *Pseudomonas* strains naturally associated with potato plants produce volatiles
1113 with high potential for inhibition of *Phytophthora infestans*. *Applied and Environmental*
1114 *Microbiology* **81**, 821–830. DOI: 10.1128/AEM.02999-14.
1115 60. Hultberg, M., Bengtsson, T. and Liljeroth, E. (2010) Late blight on potato is suppressed
1116 by the biosurfactant-producing strain *Pseudomonas koreensis* 2.74 and its biosurfactant.
1117 *BioControl* **55**, 543–550. DOI: 10.1007/s10526-010-9289-7.
1118 61. Jang, J. Y., Yang, S. Y., Kim, Y. C., Lee, C. W., Park, M. S., Kim, J. C. and Kim, I. S.
1119 (2013) Identification of orfamide A as an insecticidal metabolite produced by
1120 *Pseudomonas protegens* F6. *J. Agric. Food Chem.* **61**, 6786–6791. DOI:
1121 10.1021/jf401218w.
1122 62. Alsohim, A. S., Taylor, T. B., Barrett, G. A., Gallie, J., Zhang, X.-X., Altamirano-
1123 Junqueira, A. E., Johnson, L. J., Rainey, P. B. and Jackson, R. W. (2014) The
1124 biosurfactant viscosin produced by *Pseudomonas fluorescens* SBW25 aids spreading
1125 motility and plant growth promotion. *Environmental Microbiology* **16**, 2267–2281. DOI:
1126 10.1111/1462-2920.12469.
1127 63. Straight, P. D., Willey, J. M. and Kolter, R. (2006) Interactions between *Streptomyces*
1128 *coelicolor* and *Bacillus subtilis*: Role of surfactants in raising aerial structures. *Journal of*
1129 *Bacteriology* **188**, 4918–4925. DOI: 10.1128/JB.00162-06.
1130 64. Han, J. S., Cheng, J. H., Yoon, T. M., Song, J., Rajkarnikar, A., Kim, W. G., Yoo, I. D.,
1131 Yang, Y. Y. and Suh, J. W. (2005) Biological control agent of common scab disease by
1132 antagonistic strain *Bacillus* sp. sunhua. *J. Appl. Microbiol.* **99**, 213–221. DOI:
1133 10.1111/j.1365-2672.2005.02614.x.
1134 65. de Bruijn, I., de Kock, M. J. D., Yang, M., de Waard, P., van Beek, T. A. and
1135 Raaijmakers, J. M. (2007) Genome-based discovery, structure prediction and functional
1136 analysis of cyclic lipopeptide antibiotics in *Pseudomonas* species. *Mol. Microbiol.* **63**,
1137 417–428. DOI: 10.1111/j.1365-2958.2006.05525.x.

1138 66. Nielsen, T. H., Thrane, C., Christophersen, C., Anthoni, U. and Sørensen, J. (2000)
1139 Structure, production characteristics and fungal antagonism of tensin - a new antifungal
1140 cyclic lipopeptide from *Pseudomonas fluorescens* strain 96.578. *J. Appl. Microbiol.* **89**,
1141 992–1001.
1142 67. Götze, S., Herbst-Irmer, R., Klapper, M., Görls, H., Schneider, K. R. A., Barnett, R.,
1143 Burks, T., Neu, U. and Stallforth, P. (2017) Structure, Biosynthesis, and Biological
1144 Activity of the Cyclic Lipopeptide Anikasin. *ACS Chem. Biol.* **12**, 2498–2502. DOI:
1145 10.1021/acschembio.7b00589.
1146 68. Kuiper, I., Lagendijk, E. L., Pickford, R., Derrick, J. P., Lamers, G. E. M., Thomas-Oates,
1147 J. E., Lugtenberg, B. J. J. and Bloemberg, G. V. (2004) Characterization of two
1148 *Pseudomonas putida* lipopeptide biosurfactants, putisolvin I and II, which inhibit biofilm
1149 formation and break down existing biofilms. *Mol. Microbiol.* **51**, 97–113. DOI:
1150 10.1046/j.1365-2958.2003.03751.x.
1151 69. Götze, S., Arp, J., Lackner, G., Zhang, S., Kries, H., Klapper, M., García-Altares, M.,
1152 Willing, K., Günther, M. and Stallforth, P. (2019) Structure elucidation of the
1153 syringafactin lipopeptides provides insight in the evolution of nonribosomal peptide
1154 synthetases. *Chem. Sci.* **10**, 10979–10990. DOI: 10.1039/C9SC03633D.
1155 70. Pauwelyn, E., Huang, C.-J., Ongena, M., Leclère, V., Jacques, P., Bleyaert, P.,
1156 Budzikiewicz, H., Schäfer, M. and Höfte, M. (2013) New linear lipopeptides produced by
1157 *Pseudomonas cichorii* SF1-54 are involved in virulence, swarming motility, and biofilm
1158 formation. *Mol. Plant Microbe Interact.* **26**, 585–598. DOI: 10.1094/MPMI-11-12-0258-R.
1159 71. Wang, M., Carver, J. J., Phelan, V. V., Sanchez, L. M., Garg, N., Peng, Y., Nguyen, D.
1160 D., Watrous, J., Kapono, C. A., Luzzatto-Knaan, T., Porto, C., Bouslimani, A., Melnik, A.
1161 V., Meehan, M. J., Liu, W.-T., Crüsemann, M., Boudreau, P. D., Esquenazi, E.,
1162 Sandoval-Calderón, M., Kersten, R. D., Pace, L. A., Quinn, R. A., Duncan, K. R., Hsu,
1163 C.-C., Floros, D. J., Gavilan, R. G., Kleigrewe, K., Northen, T., Dutton, R. J., Parrot, D.,
1164 Carlson, E. E., Aigle, B., Michelsen, C. F., Jelsbak, L., Sohlenkamp, C., Pevzner, P.,
1165 Edlund, A., McLean, J., Piel, J., Murphy, B. T., Gerwick, L., Liaw, C.-C., Yang, Y.-L.,

1166 Humpf, H.-U., Maansson, M., Keyzers, R. A., Sims, A. C., Johnson, A. R., Sidebottom,
1167 A. M., Sedio, B. E., Klitgaard, A., Larson, C. B., P, C. A. B., Torres-Mendoza, D.,
1168 Gonzalez, D. J., Silva, D. B., Marques, L. M., Demarque, D. P., Pociute, E., O'Neill, E.
1169 C., Briand, E., Helfrich, E. J. N., Granatosky, E. A., Glukhov, E., Ryffel, F., Houson, H.,
1170 Mohimani, H., Kharbush, J. J., Zeng, Y., Vorholt, J. A., Kurita, K. L., Charusanti, P.,
1171 McPhail, K. L., Nielsen, K. F., Vuong, L., Elfeki, M., Traxler, M. F., Engene, N., Koyama,
1172 N., Vining, O. B., Baric, R., Silva, R. R., Mascuch, S. J., Tomasi, S., Jenkins, S.,
1173 Macherla, V., Hoffman, T., Agarwal, V., Williams, P. G., Dai, J., Neupane, R., Gurr, J.,
1174 Rodríguez, A. M. C., Lamsa, A., Zhang, C., Dorrestein, K., Duggan, B. M., Almaliti, J.,
1175 Allard, P.-M., Phapale, P., Nothias, L.-F., Alexandrov, T., Litaudon, M., Wolfender, J.-L.,
1176 Kyle, J. E., Metz, T. O., Peryea, T., Nguyen, D.-T., VanLeer, D., Shinn, P., Jadhav, A.,
1177 Müller, R., Waters, K. M., Shi, W., Liu, X., Zhang, L., Knight, R., Jensen, P. R., Palsson,
1178 B. O., Pogliano, K., Linington, R. G., Gutiérrez, M., Lopes, N. P., Gerwick, W. H., Moore,
1179 B. S., Dorrestein, P. C. and Bandeira, N. (2016) Sharing and community curation of
1180 mass spectrometry data with Global Natural Products Social Molecular Networking. *Nat.*
1181 *Biotechnol.* **34**, 828–837. DOI: 10.1038/nbt.3597.
1182 72. Aron, A. T., Gentry, E. C., McPhail, K. L., Nothias, L.-F., Nothias-Esposito, M.,
1183 Bouslimani, A., Petras, D., Gauglitz, J. M., Sikora, N., Vargas, F., van der Hooft, J. J. J.,
1184 Ernst, M., Kang, K. B., Aceves, C. M., Caraballo-Rodríguez, A. M., Koester, I., Weldon,
1185 K. C., Bertrand, S., Roullier, C., Sun, K., Tehan, R. M., Boya P, C. A., Christian, M. H.,
1186 Gutiérrez, M., Ulloa, A. M., Tejeda Mora, J. A., Mojica-Flores, R., Lakey-Beitia, J.,
1187 Vásquez-Chaves, V., Zhang, Y., Calderón, A. I., Tayler, N., Keyzers, R. A., Tugizimana,
1188 F., Ndlovu, N., Aksenov, A. A., Jarmusch, A. K., Schmid, R., Truman, A. W., Bandeira,
1189 N., Wang, M. and Dorrestein, P. C. (2020) Reproducible molecular networking of
1190 untargeted mass spectrometry data using GNPS. *Nat Protoc* **15**, 1954–1991. DOI:
1191 10.1038/s41596-020-0317-5.

1192 73. Flardh, K. and Buttner, M. J. (2009) *Streptomyces* morphogenetics: dissecting
1193 differentiation in a filamentous bacterium. *Nat Rev Micro* **7**, 36–49. DOI:
1194 10.1038/nrmicro1968.
1195 74. Choi, K.-H., Gaynor, J. B., White, K. G., Lopez, C., Bosio, C. M., Karkhoff-Schweizer, R.
1196 R. and Schweizer, H. P. (2005) A Tn7-based broad-range bacterial cloning and
1197 expression system. *Nat. Meth.* **2**, 443–448. DOI: 10.1038/nmeth765.
1198 75. Rokni-Zadeh, H., Li, W., Sanchez-Rodriguez, A., Sinnaeve, D., Rozenski, J., Martins, J.
1199 C. and De Mot, R. (2012) Genetic and functional characterization of cyclic lipopeptide
1200 white-line-inducing principle (WLIP) production by rice rhizosphere isolate
1201 *Pseudomonas putida* RW10S2. *Applied and Environmental Microbiology* **78**, 4826–
1202 4834. DOI: 10.1128/AEM.00335-12.
1203 76. Siddiqui, I. A., Shaukat, S. S., Sheikh, I. H. and Khan, A. (2006) Role of cyanide
1204 production by *Pseudomonas fluorescens* CHA0 in the suppression of root-knot
1205 nematode, *Meloidogyne javanica* in tomato. *World J. Microbiol. Biotechnol.* **22**, 641–650.
1206 DOI: 10.1007/s11274-005-9084-2.
1207 77. Ugidos, A., Morales, G., Rial, E., Williams, H. D. and Rojo, F. (2008) The coordinate
1208 regulation of multiple terminal oxidases by the *Pseudomonas putida* ANR global
1209 regulator. *Environmental Microbiology* **10**, 1690–1702. DOI: 10.1111/j.1462-
1210 2920.2008.01586.x.
1211 78. Comolli, J. C. and Donohue, T. J. (2002) *Pseudomonas aeruginosa* RoxR, a response
1212 regulator related to *Rhodobacter sphaeroides* PrrA, activates expression of the cyanide-
1213 insensitive terminal oxidase. *Mol. Microbiol.* **45**, 755–768. DOI: 10.1046/j.1365-
1214 2958.2002.03046.x.
1215 79. Feigl, F. and Anger, V. (1966) Replacement of benzidine by copper ethylacetoacetate
1216 and tetra base as spot-test reagent for hydrogen cyanide and cyanogen. *Analyst* **91**,
1217 282–284. DOI: 10.1039/AN9669100282.
1218 80. Tschowri, N., Schumacher, M. A., Schlimpert, S., Chinnam, N. B., Findlay, K. C.,
1219 Brennan, R. G. and Buttner, M. J. (2014) Tetrameric c-di-GMP mediates effective

1220 transcription factor dimerization to control *Streptomyces* development. *Cell* **158**, 1136–
1221 1147. DOI: 10.1016/j.cell.2014.07.022.
1222 81. Andrade, M. H. M. L., Niederheitmann, M., de Paula Ribeiro, S. R. R., Oliveira, L. C.,
1223 Pozza, E. A. and Pinto, C. A. B. P. (2019) Development and validation of a standard
1224 area diagram to assess common scab in potato tubers. *Eur J Plant Pathol* **154**, 739–
1225 750. DOI: 10.1007/s10658-019-01697-z.
1226 82. Nowicki, M., Foolad, M. R., Nowakowska, M. and Kozik, E. U. (2011) Potato and
1227 Tomato Late Blight Caused by *Phytophthora infestans*: An Overview of Pathology and
1228 Resistance Breeding. *Plant Dis* **96**, 4–17. DOI: 10.1094/PDIS-05-11-0458.
1229 83. Folders, J., Algra, J., Roelofs, M. S., van Loon, L. C., Tommassen, J. and Bitter, W.
1230 (2001) Characterization of *Pseudomonas aeruginosa* chitinase, a gradually secreted
1231 protein. *Journal of Bacteriology* **183**, 7044–7052. DOI: 10.1128/JB.183.24.7044-
1232 7052.2001.
1233 84. Laarman, A. J., Bardoel, B. W., Ruyken, M., Fernie, J., Milder, F. J., van Strijp, J. A. G.
1234 and Rooijakkers, S. H. M. (2012) *Pseudomonas aeruginosa* alkaline protease blocks
1235 complement activation via the classical and lectin pathways. *J. Immunol.* **188**, 386–393.
1236 DOI: 10.4049/jimmunol.1102162.
1237 85. Kenney, G. E., Dassama, L. M. K., Pandelia, M.-E., Gizzi, A. S., Martinie, R. J., Gao, P.,
1238 DeHart, C. J., Schachner, L. F., Skinner, O. S., Ro, S. Y., Zhu, X., Sadek, M., Thomas,
1239 P. M., Almo, S. C., Bollinger, J. M., Krebs, C., Kelleher, N. L. and Rosenzweig, A. C.
1240 (2018) The biosynthesis of methanobactin. *Science* **359**, 1411–1416. DOI:
1241 10.1126/science.aap9437.
1242 86. Ting, C. P., Funk, M. A., Halaby, S. L., Zhang, Z., Gonen, T. and van der Donk, W. A.
1243 (2019) Use of a scaffold peptide in the biosynthesis of amino acid-derived natural
1244 products. *Science* **365**, 280–284. DOI: 10.1126/science.aau6232.
1245 87. Clark, I. C., Melnyk, R. A., Iavarone, A. T., Novichkov, P. S. and Coates, J. D. (2014)
1246 Chlorate reduction in *Shewanella algae* ACDC is a recently acquired metabolism

1247 characterized by gene loss, suboptimal regulation and oxidative stress. *Mol. Microbiol.*
1248 **94**, 107–125. DOI: 10.1111/mmi.12746.
1249 88. Sarkisova, S. A., Lotlikar, S. R., Guragain, M., Kubat, R., Cloud, J., Franklin, M. J. and
1250 Patrauchan, M. A. (2014) A *Pseudomonas aeruginosa* EF-hand protein, EfhP (PA4107),
1251 modulates stress responses and virulence at high calcium concentration. *PLoS ONE* **9**,
1252 e98985. DOI: 10.1371/journal.pone.0098985.
1253 89. Price, M. N., Wetmore, K. M., Waters, R. J., Callaghan, M., Ray, J., Liu, H., Kuehl, J. V.,
1254 Melnyk, R. A., Lamson, J. S., Suh, Y., Carlson, H. K., Esquivel, Z., Sadeeshkumar, H.,
1255 Chakraborty, R., Zane, G. M., Rubin, B. E., Wall, J. D., Visel, A., Bristow, J., Blow, M. J.,
1256 Arkin, A. P. and Deutschbauer, A. M. (2018) Mutant phenotypes for thousands of
1257 bacterial genes of unknown function. *Nature* **557**, 503–509. DOI: 10.1038/s41586-018-
1258 0124-0.
1259 90. Mavrodi, O. V., Mavrodi, D. V., Parejko, J. A., Thomashow, L. S. and Weller, D. M.
1260 (2012) Irrigation differentially impacts populations of indigenous antibiotic-producing
1261 *Pseudomonas* spp. in the rhizosphere of wheat. *Applied and Environmental*
1262 *Microbiology* **78**, 3214–3220. DOI: 10.1128/AEM.07968-11.
1263 91. Mavrodi, D. V., Mavrodi, O. V., Elbourne, L. D. H., Tetu, S., Bonsall, R. F., Parejko, J.,
1264 Yang, M., Paulsen, I. T., Weller, D. M. and Thomashow, L. S. (2018) Long-Term
1265 Irrigation Affects the Dynamics and Activity of the Wheat Rhizosphere Microbiome. *Front*
1266 *Plant Sci* **9**, 345. DOI: 10.3389/fpls.2018.00345.
1267 92. Beskrovnaya, P., Melnyk, R. A., Liu, Z., Liu, Y., Higgins, M. A., Song, Y., Ryan, K. S.
1268 and Haney, C. H. (2020) Comparative Genomics Identified a Genetic Locus in Plant-
1269 Associated *Pseudomonas* spp. That Is Necessary for Induced Systemic Susceptibility.
1270 *MBio* **11**, 356. DOI: 10.1128/mBio.00575-20.
1271 93. Mullins, A. J., Murray, J. A. H., Bull, M. J., Jenner, M., Jones, C., Webster, G., Green, A.
1272 E., Neill, D. R., Connor, T. R., Parkhill, J., Challis, G. L. and Mahenthiralingam, E. (2019)
1273 Genome mining identifies cepacin as a plant-protective metabolite of the biopesticidal

1274 bacterium *Burkholderia ambifaria*. *Nature Microbiology* **4**, 996–1005. DOI:
1275 10.1038/s41564-019-0383-z.
1276 94. Carrión, V. J., Perez-Jaramillo, J., Cordovez, V., Tracanna, V., de Hollander, M., Ruiz-
1277 Buck, D., Mendes, L. W., van Ijcken, W. F. J., Gómez Expósito, R., Elsayed, S. S.,
1278 Mohanraju, P., Arifah, A., van der Oost, J., Paulson, J. N., Mendes, R., van Wezel, G.
1279 P., Medema, M. H. and Raaijmakers, J. M. (2019) Pathogen-induced activation of
1280 disease-suppressive functions in the endophytic root microbiome. *Science* **366**, 606–
1281 612. DOI: 10.1126/science.aaw9285.
1282 95. Tracanna, V., Ossowicki, A., Petrus, M. L. C., Overduin, S., Terlouw, B. R., Lund, G.,
1283 Robinson, S. L., Warris, S., Schijlen, E. G. W. M., van Wezel, G. P., Raaijmakers, J. M.,
1284 Garbeva, P. and Medema, M. H. (2021) Dissecting Disease-Suppressive Rhizosphere
1285 Microbiomes by Functional Amplicon Sequencing and 10× Metagenomics. *mSystems*
1286 e0111620. DOI: 10.1128/mSystems.01116-20.
1287 96. Rijavec, T. and Lapanje, A. (2016) Hydrogen Cyanide in the Rhizosphere: Not
1288 Suppressing Plant Pathogens, but Rather Regulating Availability of Phosphate. *Front*
1289 *Microbiol* **7**, 1785. DOI: 10.3389/fmicb.2016.01785.
1290 97. Kodani, S., Hudson, M. E., Durrant, M. C., Buttner, M. J., Nodwell, J. R. and Willey, J.
1291 M. (2004) The SapB morphogen is a lantibiotic-like peptide derived from the product of
1292 the developmental gene ramS in *Streptomyces coelicolor*. *Proc. Natl. Acad. Sci. U.S.A.*
1293 **101**, 11448–11453. DOI: 10.1073/pnas.0404220101.
1294 98. Willey, J. M., Willems, A., Kodani, S. and Nodwell, J. R. (2006) Morphogenetic
1295 surfactants and their role in the formation of aerial hyphae in *Streptomyces coelicolor*.
1296 *Mol. Microbiol.* **59**, 731–742. DOI: 10.1111/j.1365-2958.2005.05018.x.
1297 99. Fukuda, T. T. H., Pereira, C. F., Melo, W. G. P., Menegatti, C., Andrade, P. H. M.,
1298 Groppo, M., Lacava, P. T., Currie, C. R. and Pupo, M. T. (2021) Insights Into the
1299 Ecological Role of *Pseudomonas* spp. in an Ant-plant Symbiosis. *Front Microbiol* **12**,
1300 621274. DOI: 10.3389/fmicb.2021.621274.

1301 100. Helfrich, E. J. N., Vogel, C. M., Ueoka, R., Schäfer, M., Ryffel, F., Müller, D. B., Probst,
1302 S., Kreuzer, M., Piel, J. and Vorholt, J. A. (2018) Bipartite interactions, antibiotic
1303 production and biosynthetic potential of the *Arabidopsis* leaf microbiome. *Nature*
1304 *Microbiology* **3**, 909–919. DOI: 10.1038/s41564-018-0200-0.
1305 101. Bakker, P. A. H. M., Pieterse, C. M. J. and van Loon, L. C. (2007) Induced Systemic
1306 Resistance by Fluorescent *Pseudomonas* spp. *Phytopathology* **97**, 239–243. DOI:
1307 10.1094/PHYTO-97-2-0239.
1308 102. Teixeira, P. J. P. L., Colaianni, N. R., Law, T. F., Conway, J. M., Gilbert, S., Li, H.,
1309 Salas-González, I., Panda, D., Del Risco, N. M., Finkel, O. M., Castrillo, G.,
1310 Mieczkowski, P., Jones, C. D. and Dangl, J. L. (2021) Specific modulation of the root
1311 immune system by a community of commensal bacteria. *Proc. Natl. Acad. Sci. U.S.A.*
1312 **118**. DOI: 10.1073/pnas.2100678118.
1313 103. Xu, L., Naylor, D., Dong, Z., Simmons, T., Pierroz, G., Hixson, K. K., Kim, Y.-M., Zink, E.
1314 M., Engbrecht, K. M., Wang, Y., Gao, C., DeGraaf, S., Madera, M. A., Sievert, J. A.,
1315 Hollingsworth, J., Birdseye, D., Scheller, H. V., Hutmacher, R., Dahlberg, J., Jansson,
1316 C., Taylor, J. W., Lemaux, P. G. and Coleman-Derr, D. (2018) Drought delays
1317 development of the sorghum root microbiome and enriches for monoderm bacteria.
1318 *Proc. Natl. Acad. Sci. U.S.A.* **115**, E4284–E4293. DOI: 10.1073/pnas.1717308115.
1319 104. Santos-Medellín, C., Liechty, Z., Edwards, J., Nguyen, B., Huang, B., Weimer, B. C. and
1320 Sundaresan, V. (2021) Prolonged drought imparts lasting compositional changes to the
1321 rice root microbiome. *Nat. Plants* **7**, 1065–1077. DOI: 10.1038/s41477-021-00967-1.
1322 105. van der Meij, A., Worsley, S. F., Hutchings, M. I. and van Wezel, G. P. (2017) Chemical
1323 ecology of antibiotic production by actinomycetes. *FEMS Microbiol Rev* **41**, 392–416.
1324 DOI: 10.1093/femsre/fux005.
1325 106. Miller, J. H. (1972) Experiments in Molecular Genetics. Cold Spring Harbor Laboratory,
1326 New York.
1327 107. Kieser, T., Bibb, M. J., Buttner, M. J., Chater, K. F. and Hopwood, D. A. (2000) Practical
1328 *Streptomyces* Genetics. John Innes Foundation, Norwich.

1329 108. King, E. O., Ward, M. K. and Raney, D. E. (1954) Two simple media for the
1330 demonstration of pyocyanin and fluorescin. *J. Lab. Clin. Med.* **44**, 301–307.
1331 109. Caporaso, J. G., Lauber, C. L., Walters, W. A., Berg-Lyons, D., Lozupone, C. A.,
1332 Turnbaugh, P. J., Fierer, N. and Knight, R. (2011) Global patterns of 16S rRNA diversity
1333 at a depth of millions of sequences per sample. *Proc. Natl. Acad. Sci. U.S.A.* **108**, 4516–
1334 4522. https://doi.org/10.1073/pnas.1000080107.
1335 110. Castric, K. F. and Castric, P. A. (1983) Method for rapid detection of cyanogenic
1336 bacteria. *Applied and Environmental Microbiology* **45**, 701–702.
1337 111. Caten, C. E. and Jinks, J. L. (1968) Spontaneous variability of single isolates of
1338 *Phytophthora infestans*. I. Cultural variation. *Canadian Journal of Botany* **46**, 329–348.
1339 DOI: 10.1139/b68-055.
1340 112. Zimin, A. V., Marçais, G., Puiu, D., Roberts, M., Salzberg, S. L. and Yorke, J. A. (2013)
1341 The MaSuRCA genome assembler. *Bioinformatics* **29**, 2669–2677. DOI:
1342 10.1093/bioinformatics/btt476.
1343 113. Bankevich, A., Nurk, S., Antipov, D., Gurevich, A. A., Dvorkin, M., Kulikov, A. S., Lesin,
1344 V. M., Nikolenko, S. I., Pham, S., Prjibelski, A. D., Pyshkin, A. V., Sirotkin, A. V., Vyahhi,
1345 N., Tesler, G., Alekseyev, M. A. and Pevzner, P. A. (2012) SPAdes: a new genome
1346 assembly algorithm and its applications to single-cell sequencing. *J. Comput. Biol.* **19**,
1347 455–477. DOI: 10.1089/cmb.2012.0021.
1348 114. Seemann, T. (2014) Prokka: rapid prokaryotic genome annotation. *Bioinformatics* **30**,
1349 2068–2069. DOI: 10.1093/bioinformatics/btu153.
1350 115. Hyatt, D., Chen, G.-L., Locascio, P. F., Land, M. L., Larimer, F. W. and Hauser, L. J.
1351 (2010) Prodigal: prokaryotic gene recognition and translation initiation site identification.
1352 *BMC Bioinformatics* **11**, 119. DOI: 10.1186/1471-2105-11-119.
1353 116. Parks, D. H., Imelfort, M., Skennerton, C. T., Hugenholtz, P. and Tyson, G. W. (2015)
1354 CheckM: assessing the quality of microbial genomes recovered from isolates, single
1355 cells, and metagenomes. *Genome Res.* **25**, 1043–1055. DOI: 10.1101/gr.186072.114.

1356 117. Edgar, R. C. (2004) MUSCLE: multiple sequence alignment with high accuracy and high
1357 throughput. *Nucleic Acids Research* **32**, 1792–1797. DOI: 10.1093/nar/gkh340.
1358 118. Stamatakis, A. (2014) RAxML version 8: a tool for phylogenetic analysis and post-
1359 analysis of large phylogenies. *Bioinformatics* **30**, 1312–1313. DOI:
1360 10.1093/bioinformatics/btu033.
1361 119. Miller, M. A., Schwartz, T., Pickett, B. E., He, S., Klem, E. B., Scheuermann, R. H.,
1362 Passarotti, M., Kaufman, S. and O'Leary, M. A. (2015) A RESTful API for Access to
1363 Phylogenetic Tools via the CIPRES Science Gateway. *Evol. Bioinform. Online* **11**, 43–
1364 48. DOI: 10.4137/EBO.S21501.
1365 120. Letunic, I. and Bork, P. (2021) Interactive Tree Of Life (iTOL) v5: an online tool for
1366 phylogenetic tree display and annotation. *Nucleic Acids Res.* **49**, W293–W296.
1367 https://doi.org/10.1093/nar/gkab301.
1368 121. Campilongo, R., Fung, R. K. Y., Little, R. H., Grenga, L., Trampari, E., Pepe, S.,
1369 Chandra, G., Stevenson, C. E. M., Roncarati, D. and Malone, J. G. (2017) One ligand,
1370 two regulators and three binding sites: How KDPG controls primary carbon metabolism
1371 in *Pseudomonas*. *PLoS Genet* **13**, e1006839. DOI: 10.1371/journal.pgen.1006839.
1372 122. Scott, T. A., Heine, D., Qin, Z. and Wilkinson, B. (2017) An L-threonine transaldolase is
1373 required for L-threo-β-hydroxy-α-amino acid assembly during obafluorin biosynthesis.
1374 *Nat. Commun.* **8**, 15935. DOI: 10.1038/ncomms15935.
1375 123. Shannon, P., Markiel, A., Ozier, O., Baliga, N. S., Wang, J. T., Ramage, D., Amin, N.,
1376 Schwikowski, B. and Ideker, T. (2003) Cytoscape: a software environment for integrated
1377 models of biomolecular interaction networks. *Genome Res.* **13**, 2498–2504.
1378 https://doi.org/10.1101/gr.1239303.
1379 124. Sarwar, A., Latif, Z., Zhang, S., Zhu, J., Zechel, D. L. and Bechthold, A. (2018)
1380 Biological Control of Potato Common Scab With Rare Isatropolone C Compound
1381 Produced by Plant Growth Promoting *Streptomyces* A1RT. *Front. Microbiol.* **9**, 41. DOI:
1382 10.3389/fmicb.2018.01126.

1383 125. Lin, C., Tsai, C.-H., Chen, P.-Y., Wu, C.-Y., Chang, Y.-L., Yang, Y.-L. and Chen, Y.-L.
1384 (2018) Biological control of potato common scab by *Bacillus amyloliquefaciens* Ba01.
1385 *PLoS ONE* **13**, e0196520. DOI: 10.1371/journal.pone.0196520.
1386